NTNU

Norwegian University of
Science and Technology

Characterization of mitochondrial respiration in Atlantic salmon *(Salmo salar)* fed with glutamate and succinate enhanced diet

Naveenan Manoharan

Marine Coastal Development
Submission date: July 2018
Supervisor: Rolf Erik Olsen, IBI
Co-supervisor: Bjørg Egelandsdal, NMBU
Erik Slinde, NMBU

Norwegian University of Science and Technology
Department of Biology

Acknowledgements

This Master's thesis was written at the Department of Biology, Norwegian University of Science and Technology (NTNU) for master's program of Marine Coastal Development. First and foremost, I would like to thank my main supervisor Professor Rolf Erik Olson for providing me this opportunity to work on this project. He was helpful in giving me the guidance and necessary arrangements to work on this project.

Special thanks must go to my co-supervisors, Professor Bjørg Egelandsdal, Faculty of Chemistry, Biotechnology and Food Science, Norwegian University of Life Sciences (NMBU) for providing me the accommodation and training and the use of the facilities at NMBU. Professor Erik Slinde, Institute of Marine Research, Bergen is thanked for guidance using the equipment for the experiments. I am grateful for Lene Ruud, Head engineer, Faculty of Chemistry, Biotechnology and Food Science, NMBU for spending long hours with me to teach the practical aspects of oxygraph equipment. A big thank you to BioMar AS for providing the diets for the fish in this project.

I would also like to thank my co-supervisor, Signe Dille Løvmo, PhD candidate at NTNU for helping me in maintaining and feeding the fish and giving me a helping hand during challenging times. It was a pleasure to work with you.

Thanks to Kjersti Rennan Dahl and Tora Bardal, senior engineers at NTNU Sealab for providing me the needed chemicals and teaching me to use some equipment. To all the LAKS students at Sealab for providing a friendly environment and interesting discussions. Also, my thanks go to Lisbeth Aune, student advisor at NTNU for helping me to overcome the obstacles in finishing my master thesis.

Finally, my thanks go to my parents for providing me all the necessary support and encouragement to live in Norway and engage in a master's degree.

Trondheim, May 2018

Naveenan Manoharan

Abstract

The smolt stage of salmon has challenges in reaching adequate growth rates due to the changing environmental conditions at sea. Therefore, it is necessary to provide adequate diets to achieve sufficient growth. The present experiment is focused on studying the impact of growth in smolts of Atlantic salmon fed with glutamate and succinate (1% each) supplemented diet during a one-month period. The study focuses on characterization of mitochondrial respiration capacity using high-resolution respirometry technique in salmon provided with supplementary diets. Total protein content and citrate synthase enzyme activity were also quantified in heart and liver tissues.

Results indicate that there was no statistically significant difference in growth response between the fish groups fed and not fed glutamate and succinate. Mitochondrial respiratory states showed that the addition of succinate lead to maximum OXPHOS. A significant difference was observed in LEAK respiration state in heart tissues. No significant difference was observed in the respiration states of liver tissues. Comparison of heart and liver tissue responses for substrates and inhibitors revealed significant differences. Flux control ratio between ETS and OXPHOS showed significant difference in liver homogenates. Oxygen consumption rate ratios normalized to OXPHOS showed several significant differences, therefore, revealing that responses were organ and diet dependent.

Nominally higher citrate synthase activity was observed in heart and liver tissues, although not statistically significant. Results from the present study establish the importance of both dietary succinate and glutamate supplementation in improving growth rates in smolt stages of farmed Atlantic salmon as well as producing positive changes in mitochondrial activity. Further studies on salmon mitochondrial activity in other organs has been suggested.

Keywords: mitochondrial respiration, *Salmo salar*, glutamate, succinate, fish diet, oxidative phosphorylation, oxygraph

Contents

Abbreviations

a.d.: aqua distillate (distilled water)

BSA: Bovine Serum Albumin

CI: Complex I

CII: Complex II

CoA: Coenzyme A

CS: Citrate Synthase

ETC: Electron Transport Chain

ETS: Electron Transport System

FW: Formula weight

HRR: High-Resolution Respirometry

L: LEAK respiratory state

P: Oxidative phosphorylation

ROX: Reactive oxygen consumption

Rpm: Revolutions per minute

RT: Room temperature

SEM: Standard Error Mean

SGR: Specific growth rate

SUIT: Substrate-uncoupler-inhibitor-titration

1.0 Introduction

1.1 Overview of aquaculture in Norway

Aquaculture in Norway has been a success story so far. The history of aquaculture dates back to 1850 with the hatching of first brown trout (*Salmo trutta trutta*) and importing of rainbow trout (*Oncorhynchus mykiss*) from Denmark around 1900 for startup of pond culture (FAO, 2005). A technological breakthrough was the construction of the first cage in the 1970s (FAO, 2005), thus paving the way for commercial aquaculture production in Norway (Beveridge and Grøttum, 2007). Cage culture proved to be more efficient and safer than other forms of farming methods.

Norway's long coastline comprising many islands and inlets together with the influence of Gulf stream that provides reliable temperature have ensured excellent conditions for aquaculture (Trygve, 1993). Aquaculture sites have been set up covering almost the entire coast of Norway (Lyngstad et al., 2016) mainly focused on salmon farming. Data from FAO (2016) suggest that Norwegian aquaculture production has been increasing steadily throughout the years. It is evident that the aquaculture production significantly increased during the late 2000s.

1.1.1 The significance of Norwegian salmon industry

Norway dominates the world's farmed salmon industry. FAO (2005) statistics mention that salmon and trout have become major export products from Norway. Furthermore, the technology, consultancy and fish farming equipment from Norway have also reached global markets. According to the country's national statistics (Statistics Norway, 2016), out of the produced quantity, more than 94 percent accounted for salmon production.

1.2 Lifecycle of Atlantic salmon

The distribution of Atlantic salmon is vast ranging from Portugal to North America, including rivers in Spain, UK, France, Ireland, Norway, Sweden, Finland, Iceland, some parts of Canada and the northeast of US (Mills, 1991). The reproductive and nursery phases take place in freshwater and adult development and rapid growth occur in the marine environment (Mills, 1991). This type of life cycle (figure 1.1) is known as 'anadromous'. After hatching, the development of young fish occurs in freshwater for 2 to 4 years before migrating to the ocean.

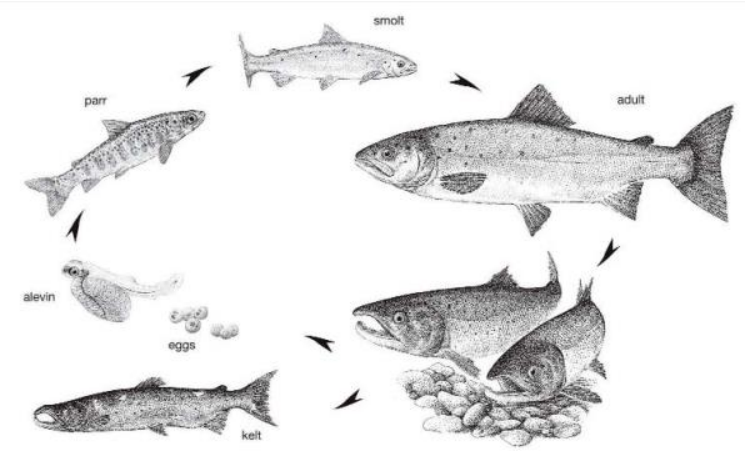

Figure 1.1: Diagrammatic representation of the Atlantic salmon life cycle (Hendry and Cragg-Hine, 2003)

Morphological changes can be seen in males and females upon returning to the freshwater environment. These changes include a darker appearance in color and variations in teeth and jaws. Spawning occurs during autumn or winter season in the excavated depressions in the river substrate known as 'redds'. The female can produce up to 1,100 eggs per kg of body weight (Hendry and Cragg-Hine, 2003). After spawning, females move downstream, and males may remain to spawn with further females.

When male and female adults return, they do not feed in freshwater. The migration and spawning lead to approximately 40% loss in body weight (Belding, 1934). The eggs hatch in spring and incubation period is dependent on water temperature (Sedgwick, 1982). Newly hatched fish (i.e. alevins) obtain nutrition from the yolk sac until they emerge to feed as fry. The fry and parr stages primarily feed upon invertebrates such as aquatic insect larvae. Parr stage exists usually for two years before smoltification[1]. Physiological, morphological and behavioral changes take place during smoltification. This generally occurs when the parr stage reaches a length between 100-120 mm (Hendry and Cragg-Hine, 2003). Fish in their smolt stage migrate to the sea, between April and June. Rapid growth can be observed during the smolt stage when salmon feed on other fish such as sapelin and sandeels, and crustacea (Shearer and Balmain, 1967). When they reach the adult stage, they return to their natal river to spawn in freshwater. This behavior of returning to their natal river is believed to take place due to the

[1] Smoltification: a series of morphological, behavioral and physiological changes that take place in salmonids during their movement from freshwater to marine environment (Folmar and Dickhoff, 1980)

fact that smolts make a note of the scents of their natal river when they migrate to the ocean (Hasler and Wisby, 1951).

1.2.1 Challenges in seawater phase of farmed Atlantic salmon

When considering the grow-out of farmed Atlantic salmon, the seawater phase can be considered as the most value-adding phase. This phase of salmon lifecycle becomes challenging due to the shifting environmental conditions during seasons (Oehme et al., 2010). Studies have shown that seasonal variation affects growth rate, feed utilization and product quality (Thorpe et al., 1989). The period after sea transfer of 1+ smolt in spring and the first spring following sea transfer for 0+ smolt during autumn are the periods that must be considered (Oehme et al., 2010). Decreased feed intake, low energy retention, decreased body energy level and condition factor have been observed (Alne et al., 2011) together with disease outbreaks (Alne et al., 2009).

1.3 Significance of glutamate and succinate in salmon diet

These challenges in the grow-out phase of Atlantic salmon can be overcome by implementing strategic dietary supplements. Studies have shown that these supplements facilitate to improve the performance of farmed fish (Burrells, Williams and Forno, 2001; Burrells, Williams, Southgate and Wadsworth, 2001; Rørvik et al., 2007). Among the strategic dietary supplements, specific amino acids have become potential candidates. In addition to being monomer compounds of proteins, amino acids have shown to hold specific functions, acting as metabolic regulators for maintenance, growth, immune response and reproduction (Meijer, 2003; Li, Mai, Trushenski and Wu, 2009). In particular, the amino acid glutamate is an important energy source in the intestine (Neu, Shenoy and Chakrabarti, 1996). Oehme et al. (2010) concluded in their study that inclusion of glutamate and arginine in aquaculture diet with supplementation levels of 1.1% and 0.75% respectively, has proved increased feeding rate, growth, and gut weight. However, another study to investigate the dietary effect of supplementing the salmon diet with glutamate showed no significant differences in growth or feed conversion ratio between the diets (Larsson et al., 2014). This study concluded that optimal dietary amino acid levels are not necessarily optimal levels for good fish health and flesh quality. A study based on micro-biota produced succinate in mice concluded that succinate activates intestinal gluconeogenesis, thus contributing to improved plasma glucose and body weight (Vadder et al.,

2016). However, no studies were found in relation to the impact of succinate on fish growth and health.

The significance of Atlantic salmon as a species in Norwegian aquaculture is evident, therefore, interests have been shown to increase the production. Although some studies have been conducted in relation to dietary supplements and fish growth no studies were found related to mitochondrial respiration and dietary supplements. The present study focused on improving mitochondrial respiration in Atlantic salmon by means of a diet supplemented with glutamate and succinate.

1.4 Introduction to mitochondria

Commonly known as “powerhouses” in eukaryotic cells, mitochondria are cellular organelles crucial to supply the much-needed energy for living organisms. It’s interesting to note that mitochondria are adaptable in terms of their shape, location, and number to fulfill the needs of the cell (Alberts et al., 2013). They contain their own inheritance material which is mtDNA and they resemble bacteria in many ways. Furthermore, they have their own apparatus for the synthesis of RNA and proteins (Campbell and Farrell, 2014). Typical mitochondria have a short cylindrical or long tubular shape with a diameter of 0.5-1.0µm and length of 2-8µm (Yamashita et al., 2016; Campbell & Farrell, 2014). However, some literature suggests slightly different measurements (figure 1.2). Several models have been proposed to explain the structure of mitochondria however, the ‘Baffle’ model has been more commonly used (Logan, 2006; Lapajne, 2015).

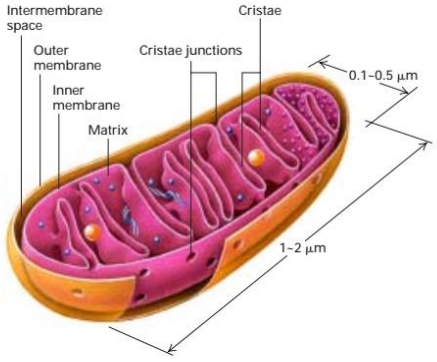

Figure 1.2: Internal structure of mitochondria based on 'Baffle' model proposed by Palade in early 1950s (Lodish et al., 2007)

Mitochondria contain 50 or more enzymes strategically located and precisely ordered in its structural components to perform energy generation and other secondary functions (Fawcett,

1981). Mitochondria consume oxygen and release carbon dioxide and this process is known as cellular respiration. The process of cellular respiration leads to the production of energy in the form of ATP and most part of this process occurs inside mitochondria. The structure of mitochondria involves a double-membrane system with inner and outer membranes with an intermembrane space present between the two membranes. The inner membrane has folds known as cristae that extend into the matrix. The matrix plays a crucial role in oxidative metabolism due to the presence of enzymes that catalyze an array of reactions. Most of the energy derived from oxidative metabolism is produced during oxidative phosphorylation that takes place in the inner membrane of mitochondria. The inner membrane is the principal site of ATP generation which is facilitated by its special structure. In addition to the increased surface area due to the presence of cristae, the inner membrane contains a high percentage of proteins involved in not only the oxidative phosphorylation but also in the transportation of metabolites (such as fatty acids and pyruvate) between cytosol and mitochondria (Cooper and Hausman, 2007). The inner membrane is impermeable to most ions and smaller molecules to maintain the proton gradient, but the outer membrane is permeable to smaller molecules. Proteins known as porins which are present in outer membrane provide channels that facilitate the free movement of molecules of 5000 daltons or less (Bruce et al., 2002).

1.5 Why mitochondria?

The interest shown by the scientific community regarding mitochondria-related research has been increasing over the past decade. The energy turnover from fat-based fish feed has been studied with the focus on growth, reproduction, feed utilization and mitochondrial enzyme activity (Eya et al., 2013). The changes in fish feed, especially in fat and protein contents have been shown to impact the mitochondria (Eya, Ashame and Pomeroy, 2010; Eya, Ashame and Pomeroy, 2011), including enzyme activity and gene expression (Eya et al., 2012). Studies have shown that aging in fish has affected mitochondrial phospholipid content and peroxidation index of most phospholipid classes (Almaida-Pagán, Lucas-Sánchez and Tocher, 2014), the decline in mitochondria DNA copy number and impairment of mitochondrial function (Hartmann et al., 2011). The energy production from mitochondria is impaired by aging (Drew et al., 2003; Desler et al., 2012; Chistiakov, Sobenin, Revin, Orekhov and Bobryshev, 2014). Fish mitochondria have a greater capacity to produce ROS (Reactive Oxygen Species) leading to oxidative stress in fish subjected to acute heat exposure (Banh et al., 2016). The fraction of cell volume occupied by mitochondria in red and white muscle fibers increased during cold

acclimation in striped sea bass (*Morone saxatilis*) (Egginton and Sidell, 1989). Cold acclimation in fish has shown a quantitative increase in muscle mitochondria (Johnston and Maitland, 1980; Tyler and Sidell, 1985). Fish in Antarctic environment possess a high and homogenous distribution of mitochondria with lower spacing between mitochondria (inter-mitochondrial space). This may be an adaptation to facilitate diffusion of metabolites under low-temperature conditions (Archer and Johnston, 1991).

1.6 The production of energy in cells

1.6.1 Catabolism

The larger molecules such as carbohydrates, proteins, and fats consumed by living organisms through their food are broken down into smaller molecules to be utilized by the cells. This process is known as catabolism (Alberts et al., 2013). Catabolism occurs in three stages (figure 1.3): the first stage involves breaking down of foods to simple subunits, the second stage involves breaking down of simple subunits to acetyl CoA and limited amounts of ATP and NADH and the final stage involves complete oxidation of acetyl CoA and production of large amounts of ATP in mitochondria. Stage one mostly occurs in the mouth and gut. Although most part of stage two occurs in the cytosol, the last part of stage two happens in the mitochondrial matrix where pyruvate is converted into acetyl groups in the presence of acetyl CoA. Stage

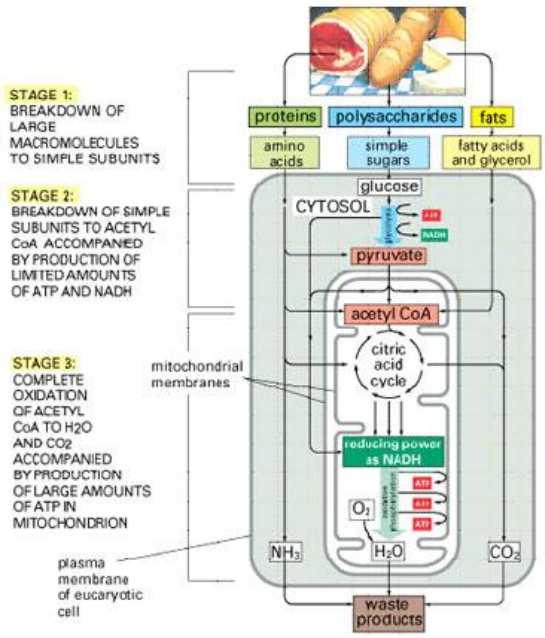

Figure 1.3: Diagrammatic representation of the three stages of catabolism (adapted from Essential Cell Biology by Alberts et al., 2013)

three starts with citric acid cycle or Krebs cycle in the mitochondrial matrix and ends with oxidative phosphorylation.

1.6.2 Krebs cycle

The reactions involved in Krebs cycle are shown in figure 1.4. The transfer of two carbon acetyl group from acetyl CoA to four carbon acceptor molecule oxaloacetate to produce six carbon citrate molecule is the beginning of Krebs cycle. Amino acids, fatty acids, and glucose can all produce acetyl CoA (Campbell and Farrell, 2014). The first step of Krebs cycle is catalyzed by the enzyme citrate synthase. The next step is the isomerization of citrate to isocitrate, catalyzed by aconitase. The third step is the oxidative decarboxylation of isocitrate to α-ketoglutarate and carbon dioxide catalyzed by isocitrate dehydrogenase. This is the first reaction where NADH is produced. Actually, this reaction occurs in two steps (Campbell and Farrell, 2014). The fourth step involves the second oxidative decarboxylation forming succinyl-CoA and carbon dioxide. An enzyme system known as α-ketoglutarate dehydrogenase complex catalyzes this reaction, which occurs in several stages. The fifth step of Krebs cycle involves the formation of succinate and CoA-SH. Also, the phosphorylation of GDP into GTP is an accompanying reaction in this step. Succinyl-CoA synthetase is the enzyme responsible for step five of Krebs cycle. The enzyme nucleoside diphosphate kinase catalyzes the transfer of a phosphate group from GTP to ADP to produce GDP and ATP. Step six involves oxidation of succinate into fumarate which is catalyzed by succinate dehydrogenase. The electron acceptor in this reaction is FAD which is reduced to $FADH_2$. Step seven involves the formation of L-malate (one of the enantiomers of malate) through a hydration reaction meaning that H_2O is added to fumarate, catalyzed by fumarase enzyme. The last step of Krebs cycle is the final oxidation step that involves regeneration of oxaloacetate by oxidizing malate into oxaloacetate. NAD^+ is reduced to NADH in this reaction. This step is catalyzed by malate dehydrogenase enzyme. Regeneration of oxaloacetate facilitates the start of another round of Krebs cycle. Two cycles will produce 6NADH, $2FADH_2$ and 2ATP. It is evident that only smaller amounts of ATP are produced from Krebs cycle. Therefore, there is a need for production of more energy for the cells to function. The process known as oxidative phosphorylation contributes to large amounts of ATP synthesis, thus significantly contributing to the energy requirement of the cells.

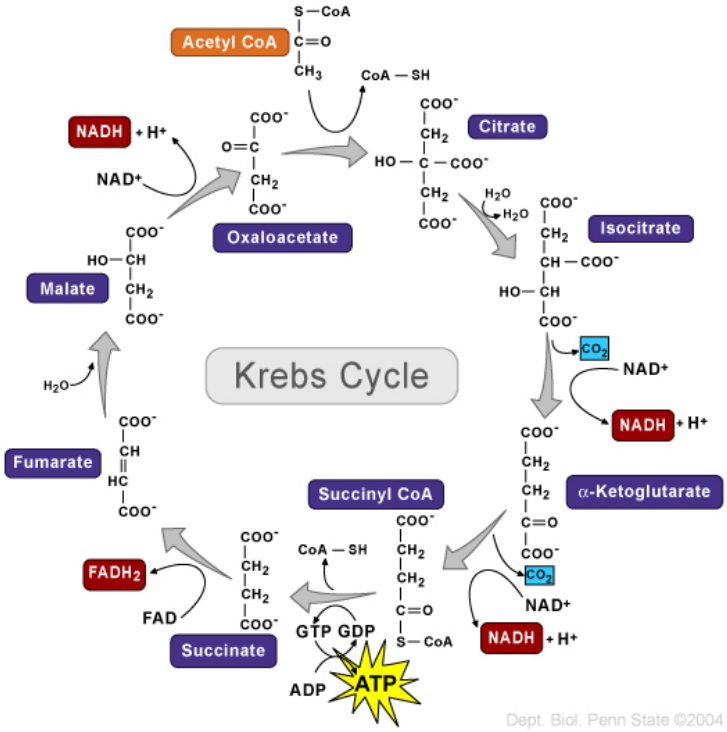

Figure 1.4: A diagram of Krebs cycle shown with main compounds and sub-compounds. Two cycles of Krebs cycle occur for every molecue of glucose. (Source: Chegg study.com)

1.6.3 Oxidative phosphorylation

Oxidative phosphorylation includes electron transport chain and chemiosmosis. The electron transport chain (ETC) is the movement of electrons through the complexes (figure 1.5) and finally being accepted by oxygen molecule. The reactions of electron transport chain occur in the inner membrane of mitochondria. Chemiosmosis involves the production of ATP. The electron transport chain and energy production are inter-related processes.

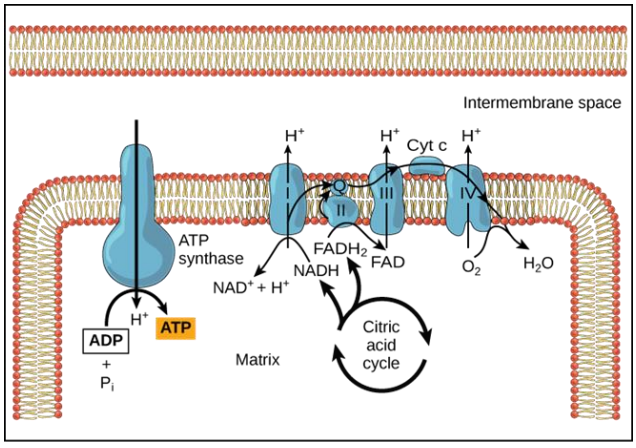

Figure 1.5: The electron transport chain and ATP production. The complexes are usually represented in roman numerals as CI- CIV. Coenzyme Q is represented with letter Q. Cyt C refers to cytochrome C. NADH and $FADH_2$ produced from Krebs cycle become electron donors. The oxygen which is the electron acceptor is reduced to water molecule (Source: OpenStax College, 2013)

Due to this inter-related nature, it is possible to mention that the production of energy consists of two stages: stage 1 and stage 2 (Alberts et al., 2013). During stage 1, high energy electrons are derived from the oxidation of food molecules and transported along electron carriers this is known as electron transport chain. The electron transport chain is a collection of reactions (figure 1.5) in which electrons from NADH and $FADH_2$ molecules (products of glycolysis and citric acid cycle) are transferred to oxygen. During stage 2, energy is produced in the form of ATP.

In addition to the movement of electrons, a proton gradient exists between the matrix and intermembrane space of mitochondria. Higher concentration of protons (H^+) in the intermembrane space leads to the proton flow towards the matrix. This flow occurs through ATP synthase; the embedded enzyme in the inner membrane (Bruce et al., 2002). The protons that reach the matrix are transported against the proton gradient back to the intermembrane space using the paths provided by the complexes. The energy required for this process is obtained from the movement of electrons since energy is released when electrons move through the respiratory complexes.

1.6.4 Respiratory complexes and their roles in electron transport chain

Each complex in ETC has its own function and components.

Complex I: the first complex is known as NADH-CoQ oxidoreductase which catalyzes the transfer of electrons from NADH to coenzyme Q (CoQ). The complex is part of the inner mitochondrial membrane and it includes subunits such as several proteins containing iron-sulfur clusters and flavoprotein that are required for oxidizing NADH (Campbell and Farrell, 2014). The substrates glutamate, malate and pyruvate provide electrons into complex I (Gnaiger, 2014a). Complex I is involved in the movement of protons from the matrix towards the intermembrane space.

Complex II: the second complex is succinate-CoQ oxidoreductase which also catalyzes the transfer of electrons from succinate (from Krebs cycle) to coenzyme Q (Campbell and Farrell, 2014). There is not enough energy generated in this reaction to drive ATP production and it does not contribute to H^+ transport across mitochondria membrane (Campbell and Farrell, 2014).

Complex III: $CoQH_2$-cytochrome c oxidoreductase also known as cytochrome reductase catalyzes the oxidation of reduced coenzyme Q ($CoQH_2$). The electrons produced in this reaction are passed along to cytochrome C in several steps. Coenzyme Q and cytochrome C are not part of the respiratory complex, but they can move freely in the membrane (Campbell and Farrell, 2014). The oxidation of coenzyme Q needs two electrons and the reduction of Fe(III) to Fe(II) needs only one electron (Campbell and Farrell, 2014). Hence, two molecules of cytochrome C are required for each molecule of coenzyme Q. Complex III has cytochrome b, cytochrome c1 and iron-sulfur proteins as its components (Campbell and Farrell, 2014). As similar to complex I, complex III is also involved in transporting protons from matrix to intermembrane space.

Complex IV: the fourth complex which is cytochrome C oxidase is responsible for catalyzing the final steps of electron transport. This final transport involves transferring of electrons from cytochrome C to oxygen, thereby oxidizing cytochrome C. The pumping of protons also takes place in this reaction. Protons are pumped from the matrix into the intermembrane space. This complex contains cytochromes a and a3, two Cu^{2+} ions which are involved in electron transport process (Campbell and Farrell, 2014). The reduced cytochrome oxidase gets oxidized by oxygen while the oxygen itself is reduced to water. This final electron carrier has the highest redox potential of all (Alberts et al., 2013). Four electrons are donated by cytochrome C and four protons from the aqueous environment are added to each O_2 molecule.

$$4e^- + 4H^+ + O_2 \longrightarrow 2H_2O$$

Additionally, four other protons are pumped across the membrane. This movement of electrons drives allosteric changes in the conformation of protein which moves protons out of the mitochondrial matrix. A special oxygen-binding site within this protein complex serves as the last repository for all electrons contributed by NADH during the beginning of electron transport chain.

1.6.5 Coupling and uncoupling respiration

The proton gradient and the voltage across the membrane provide the basis for the coupling mechanism which drives ATP synthesis. This mechanism is known as chemiosmotic coupling (Campbell and Farrell, 2014). The consumption of oxygen is coupled with production of ATP. However, the addition of some uncoupling agents will interrupt this coupling process. Uncouplers inhibit the coupling between the electron transport and phosphorylation reactions

thus inhibiting ATP synthesis without affecting the respiratory chain and ATP synthase (Terada, 1990).

1.7 Respiratory states

In mitochondrial preparations, there are three well-defined coupling states of respiration (Kontro, 2016): LEAK (L), OXPHOS (P) and ETS (E). The LEAK state is measured in the presence of reducing substrates, but in the absence of ADP, therefore, no ATP is synthesized. However, oxygen is consumed, and heat is produced. The OXPHOS state is the respiration at saturating concentrations of ADP and inorganic phosphate. During this respiratory state, the ATP synthesis is maximized. In this study, the maximum OXPHOS corresponds to the state after addition of succinate. The ETS state is the respiratory electron transfer system capacity which is induced by the addition of an uncoupler, meaning that the proton flow through the mitochondrial membrane is uncoupled from ATP synthesis.

1.8 Citrate synthase (CS)

Citrate synthase is a pace-maker enzyme in the Krebs cycle. It is synthesized in the cytoplasmic ribosomes and transported into the mitochondrial matrix. Citrate synthase is commonly used as a marker enzyme to analyze the content of intact mitochondria (Williams et al., 1986; Hood, Zak, and Pette, 1989). Since CS activity in a specific tissue is frequently constant when expressed per mitochondrial protein (Renner et al., 2003), it is suitable to use this enzyme to determine the intact mitochondria content in samples. CS catalyzes the following reaction with two- carbon acetyl-Coenzyme A with four-carbon oxaloacetate to form six-carbon citrate. This reaction leads to the regeneration of coenzyme A.

$$\text{Acetyl CoA} + \text{oxalacetate} + \text{H}_2\text{O} \rightarrow \text{citrate} + \text{Coenzyme A}$$

2.0 Aims of the study

The overall aim of the present study was to investigate the potential of glutamate and succinate incorporated diet in boosting the Krebs cycle performance in Atlantic salmon. The performance was evaluated in heart and liver of fish.

The following hypotheses were used to achieve the overall aim:

- Diet which includes glutamate and succinate leads to improved growth in smolt stages of Atlantic salmon
- Glutamate and succinate can help to upregulate mitochondrial respiration in salmon heart and liver

Comparisons were made between groups fed or not fed glutamate and succinate. Weight based data was used to determine the effect of glutamate and succinate on growth performance of salmon smolts.

High resolution respirometry measurements were used to test the mitochondrial respiration and to identify any significant differences between the groups. Ratios between substrates used in respirometry were used to reduce analytical errors in measurements.

Citrate synthase activity was used as a marker enzyme to test mitochondrial content in frozen heart and liver to identify any differences between the two groups. This enzyme activity was related to protein content. It was expected that glutamate and succinate will lead to increased enzyme activity, thus increased mitochondrial protein content.

3.0 Materials

3.1 Fish diet information

Two diet types were provided: control feed (BioMar AS, Norway) and an experimental diet supplemented with glutamate and succinate (BioMar AS, Denmark) consisting 1% each. The diets were provided in the form of pellets. Therefore, the experiment was focused on two groups: fish fed and not fed with glutamate and succinate.

3.2 High-resolution respirometry in mitochondrial studies

3.2.1 Introduction to oxygraph

Respirometry in a closed chamber-based environment involves determining the changes in the available oxygen concentration. A decrease in oxygen concentration is observed when the biological sample consumes oxygen. The plotting of oxygen concentration against elapsed time provides an estimate of oxygen consumption. Conventional methods for measuring oxygen consumption such as manometric and volumetric techniques were replaced by modern polarographic recording of oxygen concentration (Hütter et al., 2006). Modern techniques involve the use of high-resolution respirometry (HRR) devices that can be used to perform high resolution analysis of oxygen consumption with high sensitivity in biological samples. OROBOROS Oxygraph-2k (figure 3.1) is an HRR instrument used to study bioenergetics, clinical research, mitochondrial physiology and diagnosis of mitochondrial pathology (Gnaiger, 2011). This equipment has been used for many mitochondria-related studies (Gnaiger et al., 1998, Kuznetsov et al., 2008, Lanza and Nair, 2009). The system includes two chambers for simultaneous measurements of two samples. Two oxygraph machines were used in this study to perform simultaneous measurements from four samples. Respirometry takes place in a closed chamber by suspending the homogenate in a respiration medium (e.g. MiR05).

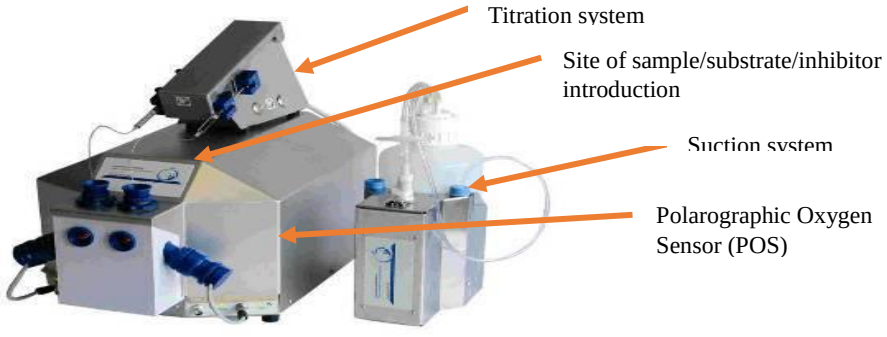

Figure 3.1: OROBOROS oxygraph-2k which includes a titration system and suctioning system to remove contents in the chambers. Two chambers are present for simultaneous measurement of two samples (Source: University of Sydney)

3.2.2 DatLab software

Data acquisition and analysis from oxygraph can be performed using DatLab software provided by Oroboros corporation. This is specifically developed for high-resolution respirometry. The program is run in computers connected to oxygraph machines. The average flux is calculated by selecting specific sections in the graphs obtained and further data processing was performed using MS Excel and statistical packages.

3.3 PBI shredder kit

The PBI-shredder kit (figure 3.2) facilitates preparation of homogenates for mitochondrial studies (Draxl, Eigentler and Gnaiger, 2015). It is a low shear mechanical homogenization

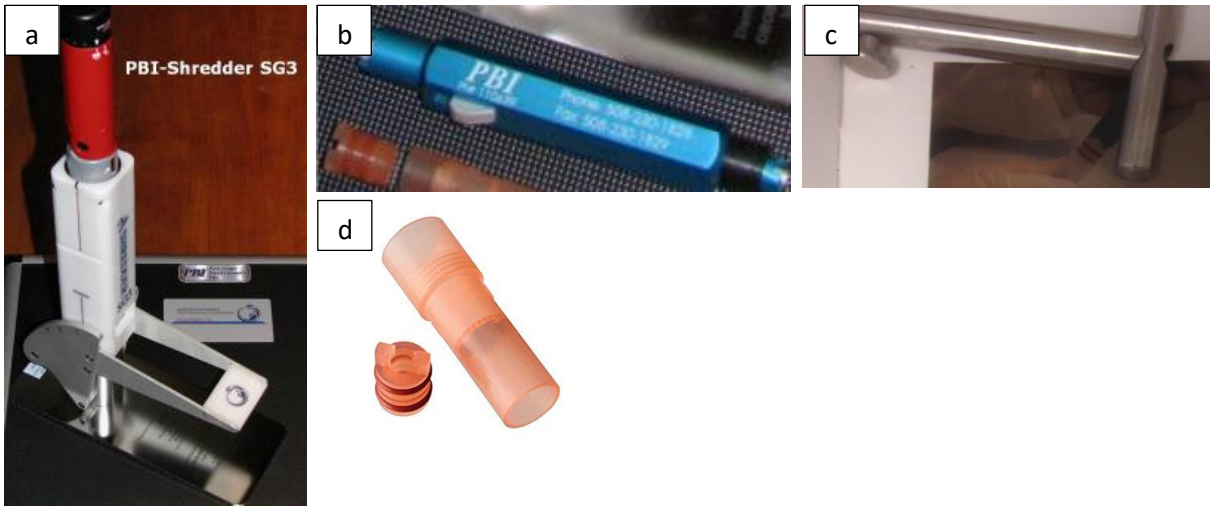

Figure 3.2: Components of PBI Shredder kit: a) PBI-Shredder SG3 (Photo: Oroboros Instruments), b) Shredder tube cap tool (Photo: Oroboros Instruments), c) shredder tube ram tool (Photo: Naveenan), d) shredder tube with cap (Photo: amazon.com)

system which is designed to apply force to the tissue in three levels (from weakest to strongest) by adjusting the lever. The PBI shredder kit includes several components: PBI-shredder SG3, shredder tubes with lysis disk, shredder rams and shredder screw caps, shredder tube cap tool and shredder tube ram tool.

3.4 Mitochondrial respiration medium

The homogenates were suspended in respiration medium (MiR05) which is a mixture of different chemicals (table 3.1). The preparation was performed by following the protocol of Oroboros (Fasching, Renner-sattler, and Gnaiger, 2016). The final pH of the medium was adjusted to 7.1 and stored at -20°C. The functional properties of the respiration medium are presented in table 3.2. Respiration medium was prepared once in large volume (5 liters) and

stored in portions of 45 ml falcon tubes at -20°C freezer. Prior to use, the falcon tubes were kept on distilled water to facilitate melting of MiR05.

Table 3.1: Chemicals used for the preparation of mitochondrial respiration medium (MiR05)

Compound name	**Final concentration**	**Formula Weight (FW)**	**Addition to 1 liter final volume**	**Supplier; storage temperature**
EGTA	0.5 mM	380.4	0.190 g	Sigma E 4378; RT
$MgCl_2 .6H_2O$	3 mM	203.3	0.610 g	Sigma M2670; RT
Lactobionic acid	60 mM	358.3 free acid	120 ml of 0.5 mM (K-lactobionate stock solution)	Aldrich 153516; RT
Taurine	20 mM	125.1	2.502 g	Sigma T 0625; RT
KH_2PO_4	10 mM	136.1	1.361 g	Merck 104873; RT
HEPES	20 mM	238.3	4.77 g	Sigma H 7523; RT
D-Sucrose	110 mM	342.3	37.65 g	Sigma S0389; RT
Bovine Serum Albumine (BSA), essentially fatty acid free	1 g/L		1 g	Sigma A6003 fraction V; 4°C

Table 3.2: Functional properties of the components in respiration medium (MiR05)

Chemical compound	**Function**
EGTA	Binder for heavy metals
$MgCl_2 .6 H_2O$	Necessary for ATPase activity
Lactobionic acid	Preserves tissue in K^+ ionic solution
Taurine	Biological membrane stabilizer
Potassium phosphate monobasic (KH_2PO_4)	Functions as a buffer in solution
HEPES	Buffer with pK value close to 7
D-Sucrose	Impermeant and oxygen radical scavenger
Bovine Serum Albumine (BSA), essentially fatty acid-free	Membrane stabilizer, binds Ca^{2+} and free fatty acids

3.5 Substrates, inhibitors and uncouplers

Addition of selected substrates, inhibitors and uncouplers to the homogenates provide information about oxygen flux during different respiratory states. Table 3.3 and table 3.4 provide chemical information and functional properties of substrate, inhibitors, and uncouplers used in this study. Table 3.5 shows the preparation method. All substrates except malonate (room temperature) were stored at -20°C. Adequate volumes of substrates were prepared in the beginning of the experiment and distributed into 2ml cryogenic tubes with labels.

Table 3.3: Substrates and inhibitors used in mitochondrial respiration capacity experiment

Chemical Name	Chemical Formula	Formula Weight	Supplier and order number	Storage temperature
L-Malic acid	$C_4H_60_5$	134.1	Sigma M 1000	RT
Adenosine 5′-diphosphate monopotassium salt dihydrate	$C_{10}H_{14}KN_5O_{10}P_2 \cdot 2H_2O$	501.3	Sigma A5285	-20 °C
Cytochrome C (from equine heart)	-	12384 Da	Sigma C7752	-20 °C
L-Glutamic acid, monosodium salt hydrate	$C_5H_8NO_4Na$	169.1	Sigma G1626	RT
Succinate disodium salt, hexahydrate	$C_4H_40_4Na_2$ $*(H_2O)_6)$	270.1	Sigma S2378	RT
Carbonyl cyanide p-trifluoro-methoxyphenyl hydrazine (FCCP)	$C_{10}H_5F_3N_4O$	254.17	Sigma C2920	4 °C
Rotenone	$C_{23}H_{22}O_6$	394.42	Sigma R8875	RT
Malonic acid	$CH_2(COOH)_2$	104.06	Sigma M1296	RT
Antimycin A from *Streptomyces* sp.	-	540	Sigma A8674	-20 °C

RT= Room temperature

Table 3.4: Substrates/inhibitors and their functions

Substrate/inhibitor	Function
Malate (L-Malic acid)	Supplying substrates for complex I
ADP	Providing energy in respiration
Cytochrome C	To test the intactness of outer mitochondrial membrane
L-Glutamic acid	Providing complex I with the substrate
Succinate	Supplying substrates for complex II
FCCP	Disabling electron transport system (ETS) from oxidative phosphorylation
Rotenone	Inhibits the transfer of electrons from Fe-S centers in complex I to ubiquinone
Malonic acid	Inhibits succinate dehydrogenase enzyme
Antimycin A	Inhibits complex III by binding to Qi site

The following table (Table 3.5) shows details about the preparation of substrates/inhibitors and uncouplers.

Table 3.5: Preparation method of substrate/inhibitor/uncoupler stock solutions and some comments

Solution	Preparation	Comments
Glutamate	1.871g/5 mL H_2O	Neutralized pH with 5N KOH
Malate	536.5mg/5 mL H_2O	Neutralized pH with 10N KOH
Succinate	1.3505g/5mL H_2O	Neutralized pH with 1N HCl
Cytochrome c	50mg/1mL H_2O	-
ADP	501.3mg/2mL H_2O	Neutralized pH with 5N KOH
Malonic acid	20.8mg/0.1mL H_2O	pH adjusted to 6 with 5M KOH
FCCP	1.27mg/5mL 99.9% ethanol	Very toxic! stored in glass vials
Rotenone	0.39mg/1mL 99.9% ethanol	Very toxic! stored in dark glass vials
Antimycin A	5.4mg/2mL 99.9% ethanol	Very toxic! stored in glass vials

*distilled water was used for preparations

3.6 Reagents used for determination of protein level

Information about the reagents used in this study to determine total protein levels based on Lowry assay (Waterborg, 2002) is shown in table 3.6. The mixture of solutions A, B and C is known as a complex-forming reagent.

Table 3.6: Ingredients and their concentrations used for determination of protein content

Ingredients	Concentration
Sodium carbonate (Na_2CO_3) - solution A	2% (w/v)
Copper(II) sulfate pentahydrate ($CuSO_4.5H_2O$) - solution B	1% (w/v)
Sodium potassium tartrate - solution C	2% (w/v)
Sodium hydroxide	2N
Folin & Ciocalteu's phenol reagent	1N
Bovine Serum Albumin fraction V	2mg/ml

3.7 Chemicals used for determination of citrate synthase activity

Information about chemicals used for CS assay is presented in table 3.7. The CS assay was performed based on the protocol suggested by Oroboros (Eigentler et al., 2015).

Table 3.7: Chemicals used for CS assay with information of stock solutions, company name, product code and storage conditions

Name	**FW**	**Stock solution**	**Company, product code, storage**
Tris(hydroxymethyl) aminomethane $C_4H_{11}NO_3$	121.14	1.0 M; 2.4228 g/20 ml a.d.	Sigma, 252859, RT
Triethanolamine $C_6H_{15}NO_3$	149.19	0.5 M; 8.06 g/100 ml a.d.	Sigma, 90279, RT
EDTA (Ethylenediaminetetra acetic acid disodium salt dehydrate) $C_{10}H_{14}N_2O_8Na_2.2H_2O$	372.20	5 mM; 186.1 mg/100 ml of 0.5 M triethanolamineHCl buffer pH 8.0	Sigma, E1644, RT
Triton X-100, $C_{34}H_{62}O_{11}$	646.87	10%; 10 g/100 ml a.d.	Sigma, T8532, 4°C
Oxaloacetic acid $C_4H_4O_5$	132.07	10 mM; 6.6 mg/5 ml of triethanolamineHCl-buffer	Sigma, O4126, -20°C
DTNB (5,5′-Dithiobis(2-nitrobenzoic acid), Ellman's reagent, $C_{14}H_8N_2O_8S_2$	396.35	1.01 mM; 2 mg/5 ml of Tris-HCl-buffer	Sigma, D8130, RT
Acetyl CoA (acetyl coenzyme A), lithium salt, $C_{23}H_{38}N_7O_{17}P_3SLi$	816.50	12.2 mM; 25 mg/2.5 ml a.d.	Sigma, A2181, -20°C
Citrate synthase (CS)		8.6 mg protein/ml	Sigma, C3260, 2-8°C

4.0 Methodology

4.1 Acclimation period of fish and diet plan

Atlantic salmon (*Salmo salar*) smolts were provided by Lerøy AS and transported in a special transport tank under optimum conditions to NTNU Sealab in Brattørkaia, Trondheim.

Gradual adaptation to seawater was performed with a slow increase of water salinity from brackish to saline conditions. The mean weight of the fish was 90 g at the time of arrival. During a one month acclimatization period, all tanks were supplied with control feed to adapt the fish to the new environment. Automatic feeders were used for feeding. Few mortalities were observed during this period which ensured favorable adaptation of the fish to the new environment. Dissolved oxygen was maintained approximately at 85-90% saturation, however, at times the oxygen levels dropped to 75-80%. The water temperature was maintained at 10-11°C. The fish were grown in six tanks: three belonging to each diet type and 25 individuals in each tank.

At the end of the acclimation period, the initial weighing of fish was performed on 19th of September 2017. The following day, three tanks were provided with experimental diet while the other three tanks were continued with the control diet. The final weighing of fish was done on 26th of October 2017. All tanks were provided with 24 hours of lighting. The feeding rate was 60g/minute.

4.1.1 Specific growth rate (SGR) analysis

Specific growth rate provided percentage increase per day. The feeding for experiment was performed for 37 days (20.09.2017 to 26.10.2017). SGR was calculated (Lugert et al., 2016) based on the following formula:

$$SGR = \left(\frac{ln(w_f) - ln(w_i)}{t}\right) \times 100$$

Where,

w_f: final weight of fish after feeding trial

w_i: initial weight of fish before feeding trial

t: number of days of feeding trial

4.2 High-resolution respirometry

4.2.1 Tissue collection and preparation

The fish were anesthetized using tricaine methanesulfonate (MS-222 Finquel®, Agent Chemical Laboratories Inc., US) and kept on ice. The apex cordis portion of heart and liver (figure 4.1) were dissected using surgical scalpel blades (Swann Morton Ltd, UK). The wet weights were measured using weighing scale (Precisa® 180A, Dietikon, Switzerland) with one decimal accuracy. The tissue sample was placed using dissecting forceps (Fisher Scientific Inc., USA) between the serrated ram and the perforated lysis disk (figure 4.2) into the pre-chilled PBI shredder tube. The ram side of shredder tube was already capped with the shredder-screw cap using the shredder-tube cap tool and it contained 500 µL respiration medium. The tissue sample was evenly distributed on the lysis disk at the narrow ram side of the shredder tube. The shredder tube was closed and placed into the pre-chilled shredder base with the ram side facing downwards (figure 4.3). Next, the shredder tube was placed into the holder of the shredder base. Shredder was activated for 30 seconds at position 1 (weakest) followed by 10 seconds at position 2 (stronger) for heart sample and 40 seconds at position 1 followed by 20 seconds at position 2 for the liver sample (figure 4.4).

Initially, trials were performed to decide the tissue size to the oxygraph. The aim of these trials was to decide the most appropriate amount of tissue to be used in the chambers based on the flux responses from substrates and inhibitors. Therefore, the amounts of tissues were decided to be 10mg of heart and 40mg of liver.

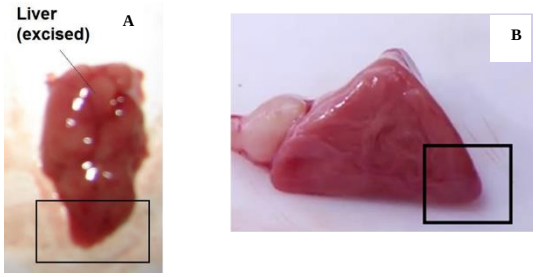

Figure 4.1: A) Portion of liver and B) portion of heart used for experiments

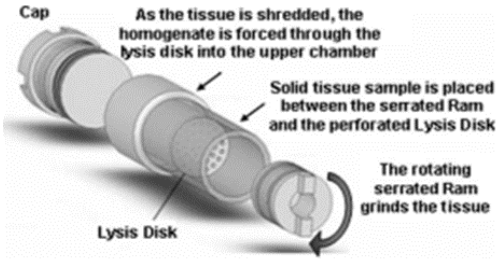

Figure 4.2: Components of shredder tube and their functions (Pressure Biosciences Inc.)

Figure 4.3: The correct positioning of the shredder tube into the shredder base with the ram side of shredder tube facing downwards

Figure 4.4: Pressing down of the driver and adjusting the lever into the suitable position

The homogenate was removed using shredder tube cap tool to unscrew the shredder-screw cap from the shredder tube by anticlockwise rotation. Next, the sample was transferred into a 50 ml falcon tube (placed on ice) using a 500 µl pipette. Then, the tube was rinsed with cold respiration medium to recover any residual sample and added into the homogenate. The shredder tube ram tool was used to open the narrow side of the shredder tube to wash any residual tissue out of the tube into the falcon tube using cold respiration medium. 3 ml of respiration medium was used to rinse and a final volume of 3.5 ml was present in the falcon tube which was intended for use with one O2k chamber. The falcon tube containing the homogenate sample was kept on ice and the next sample was prepared by following the same steps mentioned above. Once all the samples were prepared they were ready to be tested in the O2k-chambers.

Prior to the start of experiment, necessary calibrations were performed in oxygraphs according to manufacturer's protocol (Fasching and Gnaiger, 2016). Every morning before the experiment, the oxygraphs were calibrated for air saturation (figure 4.5) in the chambers for at least 30 minutes (Gnaiger, 2014b). After air calibration the respiration medium was siphoned off from the chambers using the siphoning system. The homogenate was resuspended thoroughly by pipetting six times up and down while avoiding any generation of foam. Afterwards, the homogenate in one falcon tube was inserted into one O2k-chamber. This was repeated until all the homogenates were inserted into all the chambers. i.e. four chambers in total (two oxygraphs), two chambers with heart sample and two chambers with liver sample. Once the homogenates were inserted into the chambers, the stoppers were loosely placed into the O2k-chambers to allow homogenates to warm up to the experimental temperature of 15°C.

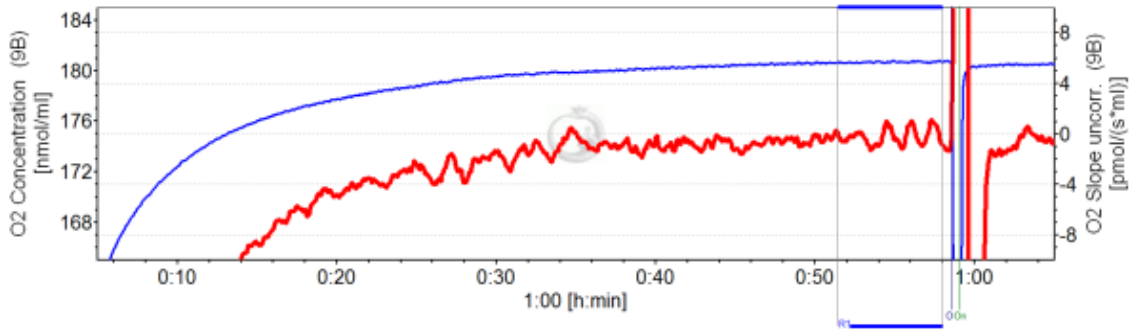

Figure 4.5: A characteristic display of air calibration shown in DatLab. Oxygen concentration (nmol/ml) is displayed in blue plot over one hour after switching on the Oxygraph-2k at a specified experimental temperature. The slope of oxygen concentration is displayed in red plot (pmol·s^{-1}·ml^{-1}) on the right Y-axis. A slope of zero indicates a constant O_2 signal. The region selected (shown in blue) between 50 minutes and 1h, which shows a constant O_2 signal was chosen to perform air calibration.

Then the chambers were closed, and excess respiration medium was siphoned off. After air calibration, the homogenates were tested for mitochondrial respiration.

4.2.2 Cleaning and maintenance of O2k chambers

Adequate cleaning of the chambers was necessary to prevent any errors in the experiment results. Therefore, proper cleaning and maintenance of the chambers was performed. The following steps were performed after each experiment:

1. The chambers were washed three times with distilled water
2. Then, they were washed one time with 70% ethanol, the stoppers were placed and left for 5 minutes
3. Afterwards, the chambers were washed two times more with 70% ethanol
4. Next, they were washed once with 100% ethanol, stoppers were placed and left for 15-20 minutes
5. Then they were washed three times with distilled water
6. The oxygraph was ready for a new experiment

At the end of an experiment day, the chambers were filled with 70% ethanol and the stoppers were placed.

4.3 The SUIT protocol

The Substrate-uncoupler-inhibitor titration (SUIT) protocol was followed with some modifications (Gnaiger, 2014a). The following order and volumes of substrates and inhibitors were used for titration to analyze mitochondrial respiration capacity: malate 25µl, ADP 25µl, cytochrome C 5µl, glutamate 50µl, succinate 25µl, FCCP 3µl, rotenone 10µl, malonate 5µl, antimycin A 10µl. For some samples, FCCP was titrated repeatedly for three times (3µl each) and antimycin A for two times (10µl each) to find stability in the flux response.

Glass syringes (Hamilton Company, US) with adequate volume capacities were used for titrations. The stable regions of the flux responses from DatLab software were considered for data analysis.

4.4 Total protein content analysis from O2k chambers

Protein levels of homogenate samples from oxygraph chambers (stored at -80°C) were determined based on Lowry assay. The following standard concentrations (table 4.1) of BSA (fraction V) were used to determine the protein concentration in the homogenate samples.

Table 4.1: Standard protein stock solutions prepared for determination of protein levels in homogenate samples (Waterborg, 2002).

Stock solution (µl)	0	2.5	5	12.5	25	50	125	250	500
Water (µl)	500	498	495	488	475	450	375	250	0
Protein concentrations (µg/ml)	0	10	20	50	100	200	500	1000	2000

0.1 ml of standard/sample was added into glass tubes (VWR International, US) followed by 0.1 ml of 2N NaOH using a pipette (Eppendorf, Germany). The glass tubes were transferred to a heating block (Techne Dri-Block DB-3D, UK) for hydrolyzation at 100°C for 10 minutes. The tubes were manually shaken during the hydrolyzation to ensure proper mixing of the components. The hydrolysates were cooled to room temperature and 1 ml of freshly mixed complex-forming reagent was added. The solutions were left at room temperature for 10 minutes followed by the addition of 0.1 ml Folin reagent using a vortex mixer (VWR® International, US). The mixture was let to stand at room temperature for 30-60 minutes. Finally,

the absorbance was recorded at 550nm wavelength using a UV-visible spectrophotometer (Varian Cary 50 Bio UV-Visible spectrophotometer, Agilent Technologies, US). A standard curve of absorbance as a function of initial protein concentration was plotted and used to determine the unknown protein concentrations in the samples.

4.5 Analysis of CS enzyme activity

CS enzyme activity was analyzed by following the protocol of Oroboros (Eigentler et al., 2015). Whole tissue samples of heart and liver were collected (n=10 from each diet type) and stored at -80°C in plastic cryogenic tubes (Sigma-Aldrich, US). Afterwards, the tissue samples were weighed (Precisa® 180A, Dietikon, Switzerland) and immediately transferred into glass test tubes (Fisher Scientific, US) placed on ice. A volume of 3.5 ml respiration medium was added into the tubes followed by homogenization (Ultra Turrax T10 basic homogenizer, IKA, Germany) for 30 seconds at level 4. A portion (2ml) of homogenized samples were transferred into microcentrifuge tubes (Fisherbrand™, Fisher Scientific, US) kept on ice. The samples were centrifuged (Biofuge Pico, Heraeus Company, Germany) at 13,000 rpm for 5 minutes. The supernatant was used to determine CS activity. The commercial citrate synthase was used as a standard to check the chemicals and assay conditions. The reaction components (table 4.2) were added in the following order (except oxalacetate solution) into a 1 ml plastic cuvette (VWR International, US). The volume of sample to be added into the plastic cuvette was decided based on table 4.2.

Table 4.2: Components and their volumes added in 1ml cuvette for CS activity measurement

	Component	**Volume added (µl)**	**Final concentration**
1	10% Triton X-100	25	˜0.25 %
2	Acetyl CoA	25	˜ 0.31 mM
3	1.01 mM DTNB	100	˜ 0.1 mM
4	V_{sample}	See table 4.3	˜ 5mg/ml
5	Distilled H_2O	(800 µl - V_{sample})	
6	Oxaloacetate	50	˜ 0.5 mM

Table 4.3: Volumes of components added into 1ml cuvette

Sample	**V_{sample} (µl)**
CS standard	5
Medium (MiR05)	10
Heart homogenate	5
Liver homogenate	10

Oxaloacetate was added immediately before the measurement of enzyme activity and the cuvette was sealed with parafilm (Sigma-Aldrich), swiveled gently three times. The parafilm was then removed and the cuvette was placed in a UV Visible spectrophotometer (Varian Cary 50 Bio UV-Visible spectrophotometer, Agilent Technologies, US). The absorbance values were measured at 412 nm wavelength. CS activity was calculated using the following equation (Eigentler et al., 2015):

Specific activity (v): $\frac{r_A}{l \cdot \varepsilon_B \cdot V_B} \cdot \frac{V_{cuvette}}{V_{sample} \cdot \rho}$

where,

v: specific activity of the enzyme measured in µmol*min^{-1}*mg^{-1}

r_A = dA/dt, rate of absorbance change (min^{-1})

l: optical path length (=1 cm)

ε_B: extinction coefficient of B (TNB) at 412 nm and pH 8.1 = 13.6 mM^{-1}*cm^{-1}

V_B: stoichiometric number of B (TNB) in the reaction (=1)

$V_{cuvette}$: volume of solution in the cuvette (= 1000 µl)

V_{sample}: volume of sample added to a cuvette (5 – 100 µl)

ρ: mass concentration or density of biological material in the sample, V_{sample} (protein concentration: mg*cm^{-3})

4.6 Statistical analysis of data

Most of the statistical analysis was performed with SPSS software version 25 (IBM Corporation, US). Shapiro-Wilk test was used to test for normality of data ($P<0.05$) prior to performing the t-test. All data were normally distributed. Independent samples t-test was used to find if there is a significant difference between the two feed groups with a confidence interval of 95% (p-value = 0.05). Graphs were produced with the software SigmaPlot version 14 (Systat Software Inc., US). Some analysis of data was performed using Microsoft Excel 2010.

5.0 Results

5.1 Fish growth

There was no statistically significant difference (P>0.05) in fish weights between control and experimental diet groups (Table 5.1). The statistical analysis was performed using independent sample t-test. The individual weights of 180 fish (90 individuals from each diet group) were measured. A nominally higher mean weight was observed in diet group without glutamate and succinate (control group) than the diet group fed glutamate and succinate (Figure 5.1). However, this was not statistically significant. Due to the reason that the fish were kept in several tanks there was a necessity to assess the growth performance of each individual tank. Hence, the Specific Growth Rate (SGR) was calculated in percentage for each tank.

Table 5.1: Mean weights ± standard error mean and standard deviation of the feed groups of Atlantic salmon used for the experiments (n= 180)

Feed Group	N	Mean Weight (g)	Standard Deviation	P-value
Control	90	191.07±3.08	29.19	0.337
Experimental	90	187.04±2.83	26.81	

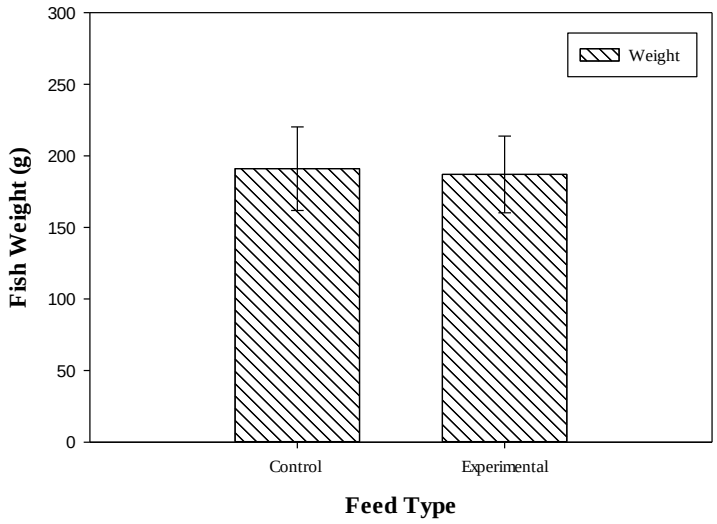

Figure 5.1: Comparison of mean weights of total fish fed with control feed and experimental feed. This graph represents the collective mean weight of all the tanks

Table 5.2: Tank based mean SGR values with standard deviation and standard error values

Tank	Diet type	N	Mean SGR values	Standard deviation	Standard error mean
A	Experimental	30	1.561	0.727	0.1330
B	Experimental	30	1.643	0.506	0.0924
C	Control	30	1.627	0.685	0.1250
D	Control	30	1.610	0.556	0.1010
E	Control	30	1.597	0.530	0.0968
F	Experimental	30	1.662	0.342	0.0624

Specific Growth Rate (SGR) analysis (table 5.2 and figure 5.2) with respect to each tank showed no statistically significant difference when compared with a p-value of 0.05. A one-way ANOVA test provided a significance value of 0.988. Although slight differences were observed in SGR among the tanks, it was evident that the growth has not been significantly affected by succinate and glutamate diet. Tanks A, B and F were fed with glutamate and succinate diet and the rest of them were controls.

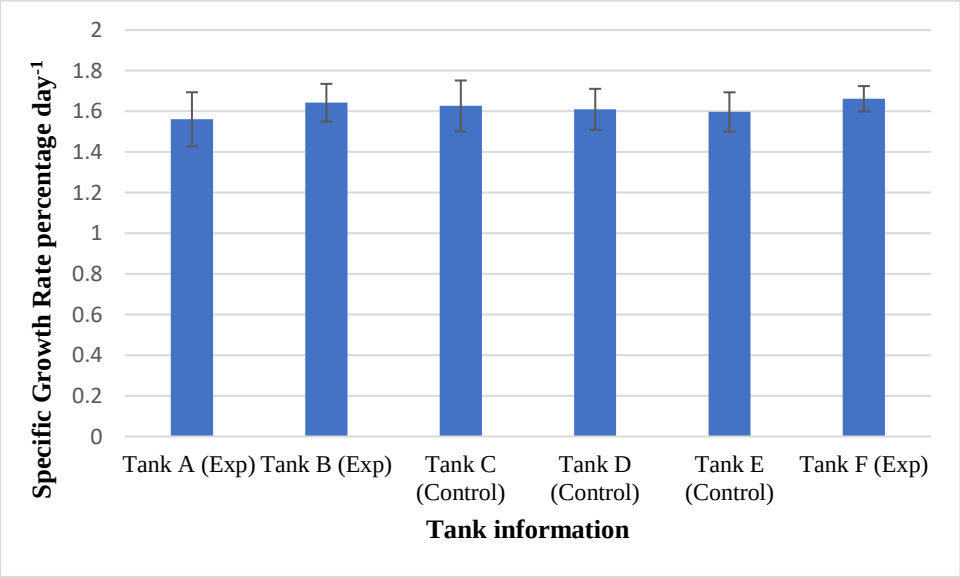

Figure 5.2: Mean SGR values based on each tank. Error bars represent standard errors.

5.2 High-resolution respirometry

5.2.1 Mitochondrial respiration capacity in heart tissue

Ten samples (n=10) were selected from each diet group to perform the independent samples t-test. The results (table 5.3) were compared with the p-value of 0.05 to conclude if there is a significant difference in flux values between the two diet groups. It was found that there was no significant difference in flux values of substrates/inhibitors between the two diet groups except for malate. The flux values of malate showed a statistically significant difference (P = 0.005). The non-parametric statistical test of Mann-Whitney was used to compare the means of ROX values due to the non-normal distribution of data. Log transformation method was used to convert non-normally distributed data into normal distribution.

Table 5.3: Mean value ± Standard Error Mean of the flux of added substrates and inhibitors in heart mitochondria of Atlantic salmon. The flux values are the tissue response to substrates/inhibitors measured in pmol/(s*ml).

Substrate/inhibitor	Control Feed	Experimental Feed	P-value
Malate	1.47± 0.08	1.01± 0.11	0.005
ADP	6.46±0.7	6.24±0.9	0.855
Cytochrome C	7.20±0.8	6.83±0.9	0.762
Glutamate	12.98±1.8	12.41±1.5	0.813
Succinate	13.30±1.9	12.90±1.6	0.872
FCCP	9.63±1.2	9.55±1.6	0.969
Rotenone	1.78±0.2	2.42±0.8	0.451
Malonate	0.54±0.2	0.38±0.1	0.454
ROX	1.08±0.3	0.53±0.09	0.212

Figures 5.3 and 5.4 are shown as examples of mitochondrial response for heart tissue. Calculations were performed by selecting the stable regions in the flux to produce histograms (figure 5.5 and 5.9). The flux values were used in SPSS (version 25) statistical software to obtain results shown in table 5.2. A histogram (figure 5.6) is presented with the flux responses from each substrate/inhibitor or uncoupler.

5.2.2 Representative O2k-traces of Atlantic salmon heart samples at 15°C temperature

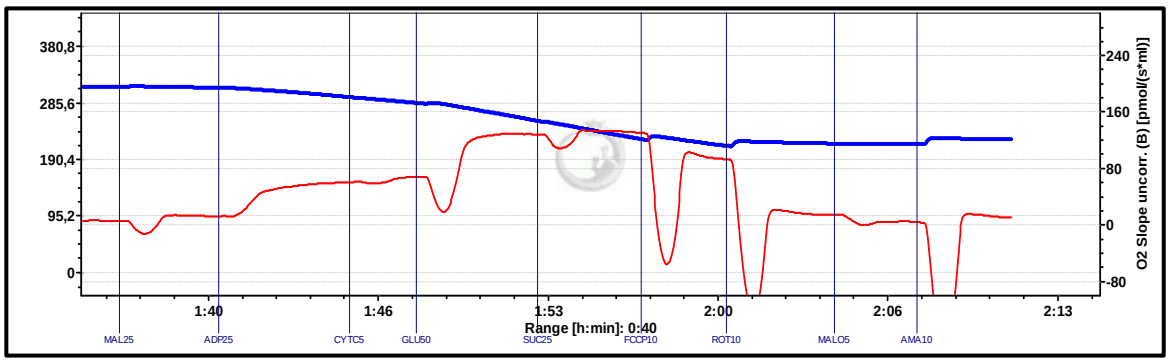

Figure 5.3: Mitochondrial response to the heart sample of salmon fed control feed. Blue trail represents oxygen concentration [nmol/ml] in the oxygraph chamber. The red trail shows the flux variation in chamber which is the response of the tissue for added substrates and inhibitors [pmol/(s*ml)] for a sample wet weight of 10mg at 15°C.

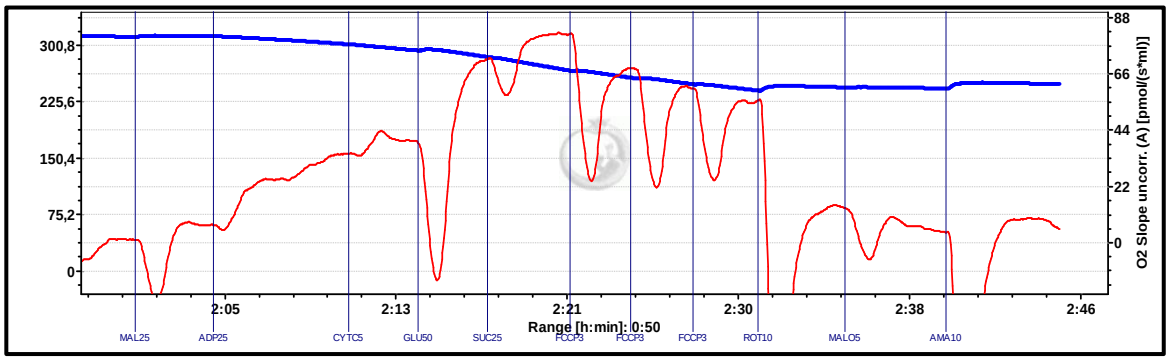

Figure 5.4: Mitochondrial response to heart sample of salmon fed with experimental feed. Blue trail represent oxygen concentration [nmol/ml] in the oxygraph chamber. The red trail shows the flux variation in chamber which is the response of the tissue for added substrates and inhibitors [pmol/(s*ml)] for a sample wet weight of 10mg at 15°C.

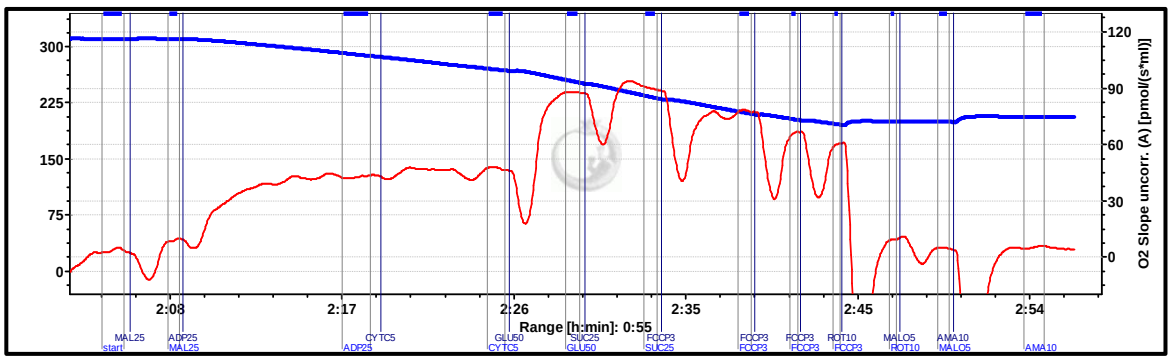

Figure 5.5: Representative diagram of heart mitochondrial response with measurement regions selected to perform further analysis. Stable regions of the flux trail (red line) were selected (shown as blue regions) to obtain flux values [pmol/(s*ml)]. Wet weight of tissue: 10mg. Malate: 0.88, ADP: 4.26, Cytochrome C: 4.75, Glutamate: 8.79, Succinate: 9.02, FCCP: 6.79, Rotenone: 0.91, Malonate: 0.48, Antimycin A: 0.51 (Flux/mg

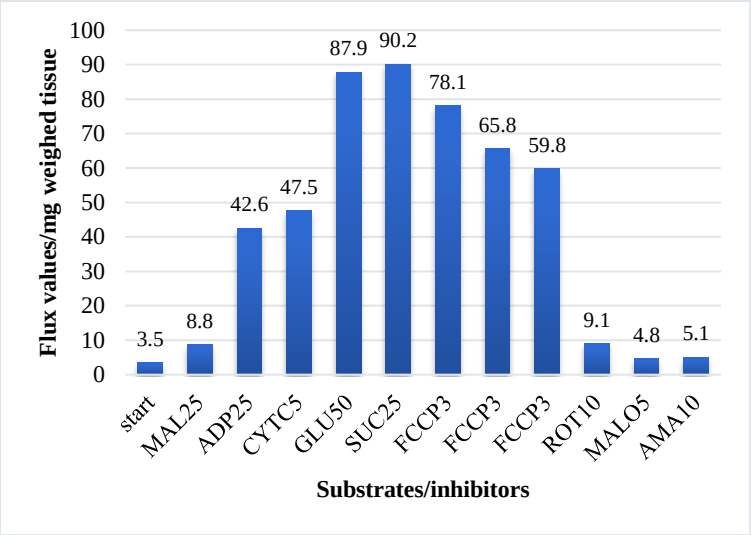

Figure 5.6: A histogram representing the flux values of added substrates/inhibitors added to the O2k chamber. The numbered labels of X axis correspond to the stable regions of the O2k trace selected in the oxygraph diagram above (Figure 5.5). The names of substrates/inhibitors in X axis are followed by the added volumes in µl. Y axis shows flux values/mg weighed tissue. MAL: malate, CYTC: cytochrome C, GLU: glutamate, SUC: succinate, ROT: rotenone, MALO: malonate, AMA: antimycin A. Subsequent additions of FCCP in 3µl each was done to try to achieve a stable flux response.

5.2.3 Mitochondrial respiration capacity in liver tissue

Ten samples (n=10) were selected from each diet group to perform independent samples t-test. The results (table 5.4) were compared with the p-value of 0.05 to conclude if there is a significant difference in flux values between the two diet groups. There was no significant difference in flux values of substrates/inhibitors.

Representative mitochondrial response for liver homogenates is shown in figures 5.7 and 5.8. Figure 5.10 shows a histogram representing flux values for a liver sample. The histogram was produced by selecting stable regions in the flux diagram obtained from O2k oxygraph.

Table 5.4: Mean value ± Standard Error Mean of the flux of added substrates and inhibitors in liver mitochondria of Atlantic salmon. The flux values are the tissue response to substrates/inhibitors measured in pmol/(s*ml).

Substrate/inhibitor	Control Feed	Experimental Feed	P-value
Malate	1.25±0.1	1.02± 0.2	0.299
ADP	1.95±0.1	1.83±0.4	0.224
Cytochrome C	2.04±0.2	1.97±0.5	0.407

Glutamate	3.18±0.3	3.36±0.8	0.663
Succinate	4.80±0.4	5.26±1.3	0.740
FCCP	4.33±0.3	4.01±0.9	0.305
Rotenone	1.64±0.1	1.76±0.4	0.798
Malonate	0.29±0.01	0.39±0.07	0.545
ROX	0.27±0.02	0.40±0.07	0.149

Statistically significant difference was observed in mean ADP response between heart and liver samples using two-way ANOVA ($p<0.05$). The response for cytochrome C addition was not very imminent, thus it confirms that the mitochondrial membrane was largely intact. Furthermore, a nominally higher succinate response was observed in the experimental diet group, consisting of glutamate and succinate enriched feed mixture than the control feed group. However, this increase was not statistically significant (P=0.731). A two-way ANOVA results showed a statistically significant difference (table 5.5) in mean succinate response between heart and liver samples.

Table 5.5: Tissue based comparison of response values for different substrates and inhibitors.

Heart vs liver	**Mean Square**	**P-value**
Malate	0.0980	0.450
ADP	3.1839	<0.05
Cytochrome C	3.2397	<0.05
Glutamate	3.6250	<0.05
Succinate	650.68	<0.05
FCCP	1.31503	<0.05
Rotenone	0.02938	0.460
Malonate	0.0364	0.615
ROX	2.1856	<0.05

As per the table 5.5, a two-way ANOVA test showed that statistically significant differences exist between heart and liver responses for substrates and inhibitors. Flux responses from malate, rotenone and malonate showed no significant differences between tissue types. Log transformation was performed to obtain normal distribution of data prior to ANOVA analysis.

ROX response values showed good predictions with non-normal distribution therefore, it was used for ANOVA without conversion into normal distribution.

5.2.4 Representative O2k-traces of Atlantic salmon liver samples at 15°C temperature

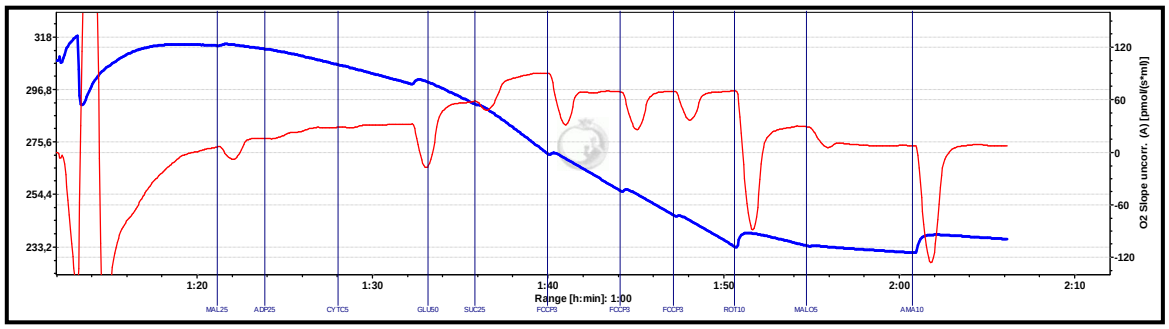

Figure 5.7: Mitochondrial response to the liver sample of salmon fed with control feed. Blue trail represents oxygen concentration [nmol/ml] in the oxygraph chamber. The red trail shows the flux variation in chamber which is the response of the tissue for added substrates and inhibitors [pmol/(s*ml)] for a sample wet weight of 40mg at 15°C.

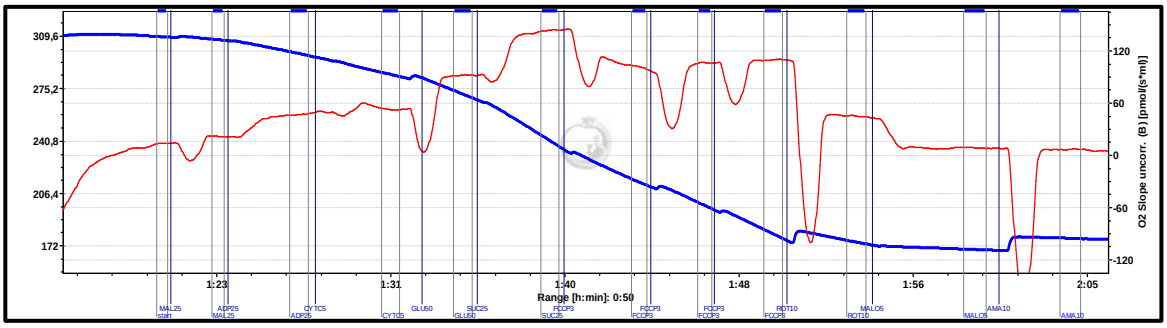

Figure 5.8: Mitochondrial response to liver sample of salmon fed with experimental feed. Blue trail represent oxygen concentration [nmol/ml] in the oxygraph chamber. The red trail shows the flux variation in chamber which is the response of the tissue for added substrates and inhibitors [pmol/(s*ml)] for a sample wet weight of 40mg at 15°C.

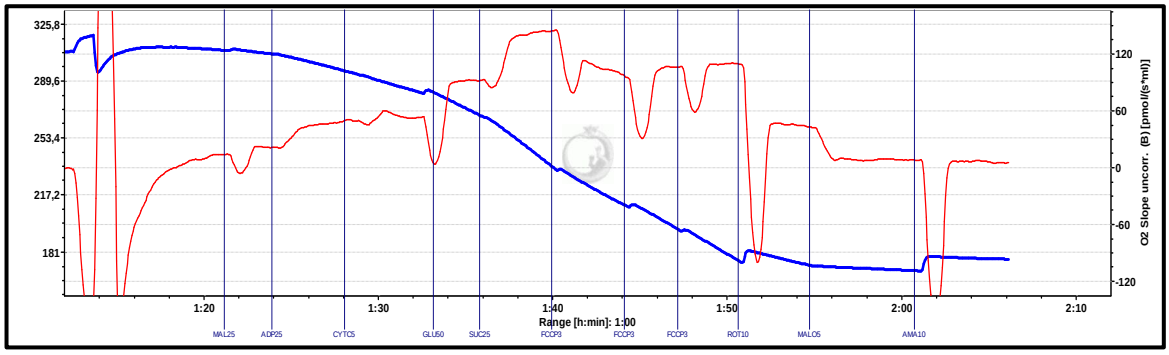

Figure 5.9: Representative diagram of liver mitochondrial response with measurement regions selected to perform further analysis. Stable regions of the flux trail (red line) were selected (shown as blue regions) to obtain flux values [pmol/(s*ml)]. Wet weight of tissue: 20mg. Malate: 1.10, ADP: 2.34, Cytochrome C: 2.64, Glutamate: 4.60, Succinate: 7.18, FCCP: 5.29, Rotenone: 2.26, Malonate: 0.44, Antimycin A: 0.35 (Flux/mg weighed tissue)

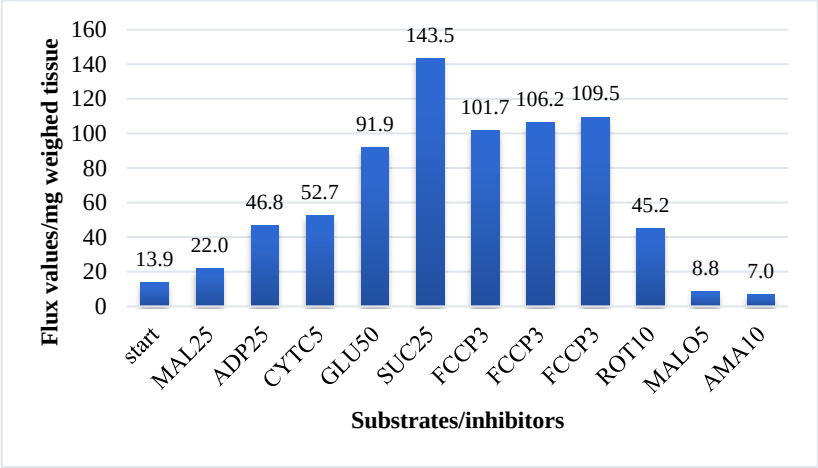

Figure 5.10: A histogram representing the flux values of added substrates/inhibitors added to the O2k chamber. The numbered labels of X axis correspond to the stable regions of the O2k trace selected in the oxygraph diagram above (figure 5.9). The names of substrates/inhibitors in X axis are followed by the added volumes in µl. Y axis shows flux values/mg weighed tissue. Y axis shows flux values/mg weighed tissue. MAL: malate, CYTC: cytochrome C, GLU: glutamate, SUC: succinate, ROT: rotenone, MALO: malonate, AMA: antimycin A. Subsequent additions of FCCP in 3µl each was done to try to achieve a stable flux response.

5.2.5 Respiratory states with respect to the tissue mass

5.2.5.1 Heart homogenates

Analysis of high-resolution respirometry data revealed a significant difference in the LEAK respiration state ($P<0.05$) between the diet groups (table 5.6). However, there was no statistically significant difference in max OXPHOS and ETS states between the diet groups). In the context of liver homogenates, there was no statistically significant difference between the diet groups (table 5.7). Respiration rate at max OXPHOS showed a slightly higher trend towards experimental diet group in liver homogenate although not statistically significant. Figures 5.11 and 5.12 represent flux control ratios normalized to maximum OXPHOS (P).

Table 5.6: Mean O_2 flux ± standard deviation at respiratory states LEAK, Max OXPHOS and ETS for heart samples (n=10) displayed in units pmol/s/mg.

Respiratory states	Control Feed	Experimental Feed	P-value
LEAK state	1.466± 0.267	1.008± 0.373	0.005
Max OXPHOS state	13.299± 5.971	12.898± 4.923	0.872
ETS state	9.631± 3.843	9.553± 4.949	0.969

Table 5.7: Mean O_2 flux ± standard deviation at respiratory states LEAK, Max OXPHOS and ETS for liver samples (n=10) displayed in units pmol/s/mg.

Respiratory states	Control Feed	Experimental Feed	P-value
LEAK state	1.253± 0.394	1.023± 0.555	0.299
Max OXPHOS state	4.801± 1.344	5.263± 3.958	0.731
ETS state	4.337±1.102	4.012± 2.905	0.745

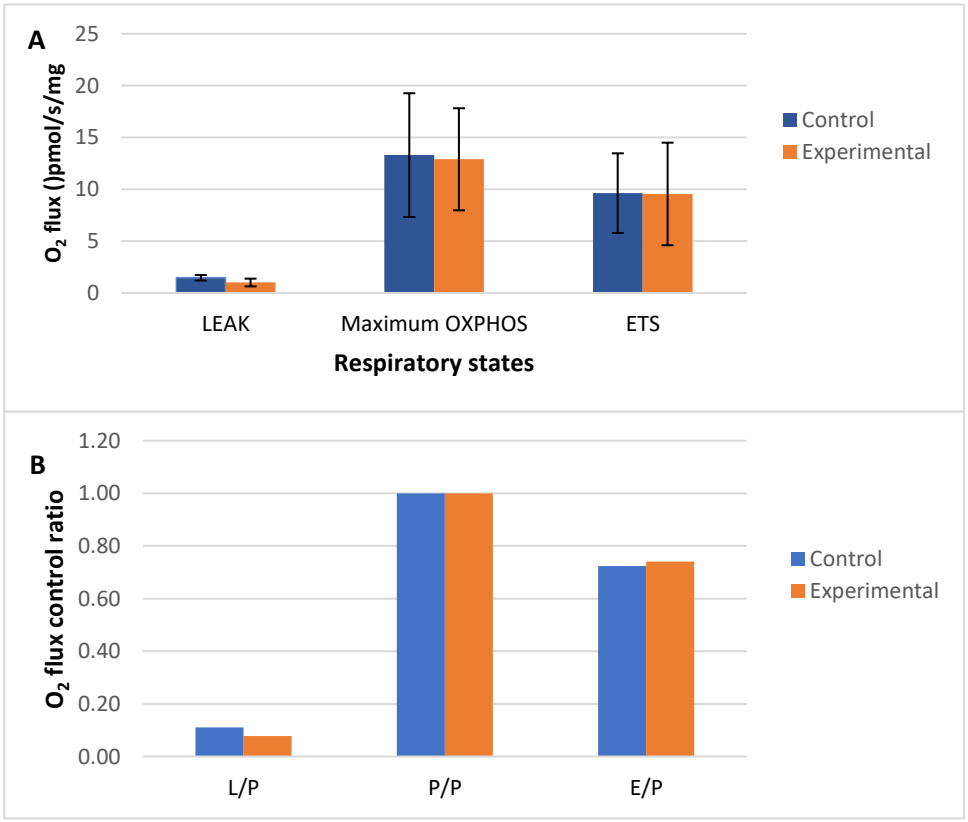

Figure 5.11: (A) Mean oxygen flux at the respiratory states L, Max OXPHOS and ETS. (B) Flux control ratio normalized to Max OXPHOS in heart samples. The error bars represent standard deviations.

There was no statistically significant difference in flux control ratios between the diet groups in heart homogenates (table 5.8). However, statistically significant difference was observed in E/P flux control ratio (table 5.9) in liver homogenates. Since ratios facilitate to reduce analytical errors, a comparison between tissue types (heart vs liver) and diet types was performed using two-way ANOVA (table 5.10). Since oxygen consumption rate (OCR) of succinate is in highest level it was considered as the OXPHOS state.

Table 5.8: Mean flux control ratios±SEM with P-values of heart homogenates

Flux control ratio	Control feed	Experimental feed	P-value
L/P	0.144±0.296	0.081±0.006	0.064
P/P	1.00±0.0	1.0±0.0	1.000
E/P	0.767±0.0435	0.733±0.061	0.663

Table 5.9: Mean flux control ratios±SEM with P-values of liver homogenates

Flux control ratio	Control feed	Experimental feed	P-value
L/P	0.879±0.613	0.223±0.0216	0.299
P/P	1.0±0.0	1.0±0.0	1.0
E/P	0.912±0.0185	0.774±0.0154	<0.05

Table 5.10: Comparison of oxygen consumption rate ratios between substrate or inhibitor /succinate for tissue types (heart vs liver) and diet types (control vs experimental)

Ratio	P-value (heart vs liver)	P-value (control vs experimental diet)
Malate/succinate	<0.05	<0.05
ADP/succinate	<0.05	0.734
Cytochrome C/succinate	<0.05	<0.05
Glutamate/succinate	<0.05	0.100
FCCP/succinate	<0.05	<0.05
Rotenone/succinate	<0.05	0.988
Malonate/succinate	<0.05	0.898
ROX/succinate	0.149	0.903

It is evident that there are significant differences between OCR ratios between the substrates and OXPHOS (succinate) with respect to tissue type and diet type. The ratios of OCR (malate)/OCR (succinate), OCR (cytochrome C)/OCR (succinate) and OCR (FCCP)/OCR (succinate) are feed dependent. In terms of OCR ratios for heart vs liver, most comparisons show statistically significant differences. Simple log transformations were necessary for most data to achieve normality.

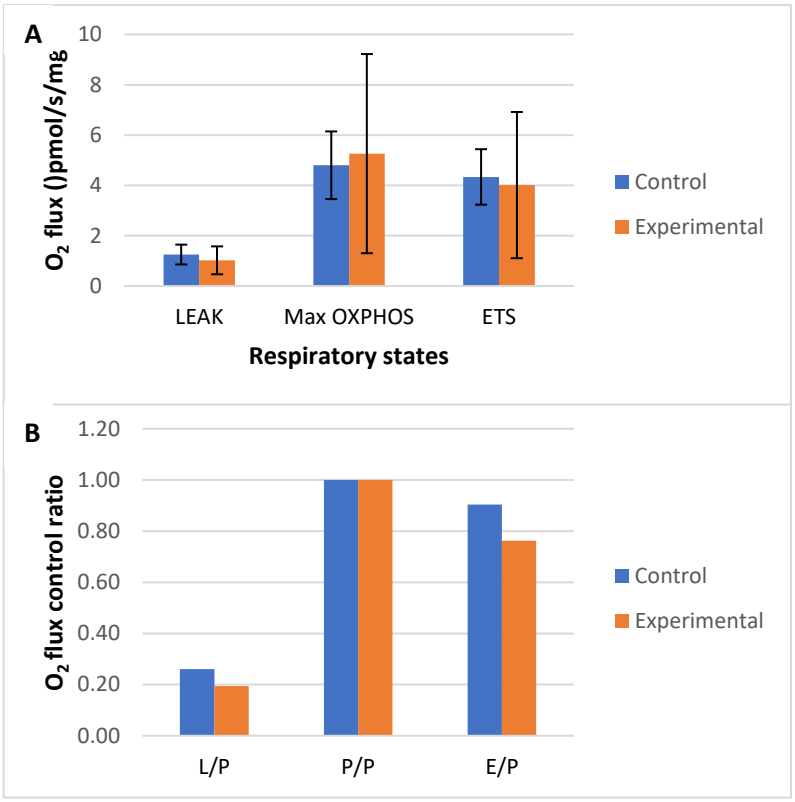

Figure 5.12: (A) Mean oxygen flux at the respiratory states L, OXPHOS and ETS. (B) Flux control ratio normalized to Max OXPHOS in liver samples. The error bars represent standard deviations.

5.3 Respiration rates normalized to protein content

5.3.1 Heart homogenates

Analysis of respiration rates (table 5.11) normalized to protein levels in O2k chambers revealed a significant difference (figure 5.13) in the ETS state. No significant differences were observed in LEAK ($P<0.05$) and maximum OXPHOS states.

Table 5.11: Respiration states normalized to protein content±SEM with P-values of heart homogenates

Respiration states	Control group	Experimental group	P-value
LEAK	0.666±0.10	0.631±0.31	0.915
Maximum OXPHOS	5.287±0.66	10.819±6.88	0.434
ETS	3.871±0.39	1.908±0.23	<0.05

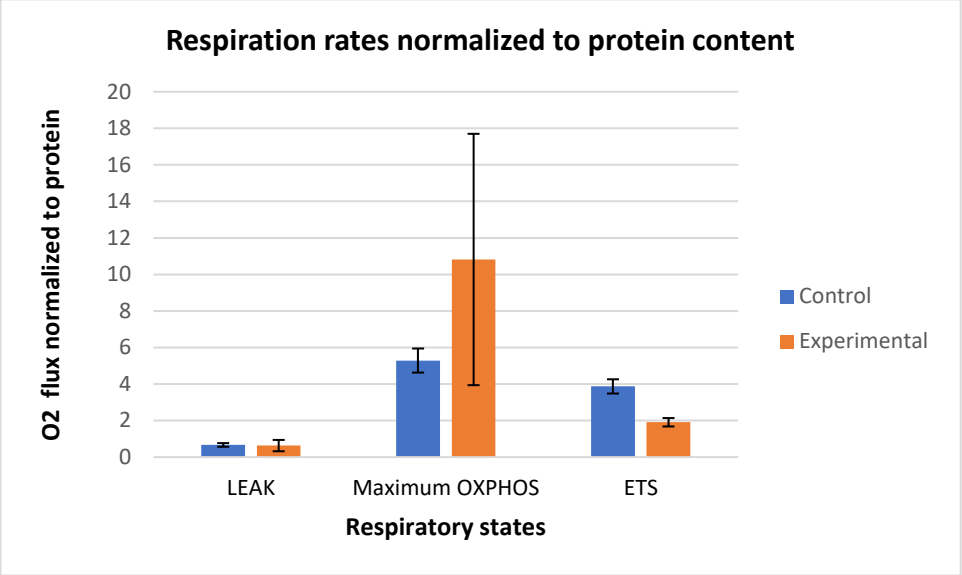

Figure 5.13: Respiration rates normalized to protein content in heart homogenate. Error bars represent standard error means.

5.3.2 Liver homogenates

Analysis of respiration rates (table 5.12) normalized to protein levels in O2k chambers revealed no statistically significant difference ($P<0.05$) in the respiration states between the diet groups (figure 5.14).

Table 5.12: Respiration states normalized to protein content±SEM with P-values of liver homogenates

Respiration states	Control group	Experimental group	P-value
LEAK	0.318±0.06	0.212±0.05	0.230
Maximum OXPHOS	1.153±0.17	1.143±0.34	0.977
ETS	1.055±0.17	0.909±0.23	0.611

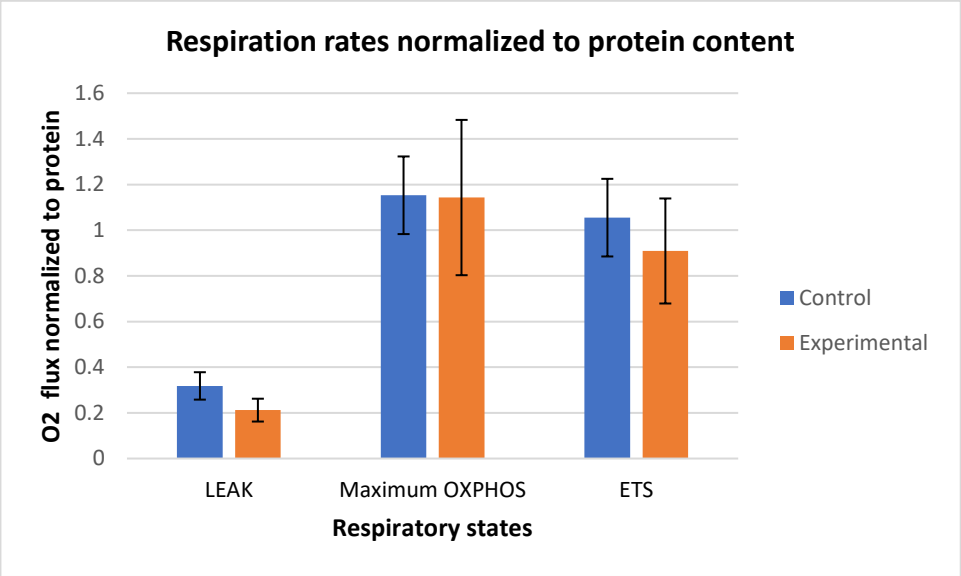

Figure 5.14: Respiration rates normalized to protein content in liver homogenate. Error bars represent standard error means.

5.4 Citrate synthase activity

5.4.1 Heart tissue samples

Statistical analysis of CS activity in tissue slices of heart samples (table 5.13 and figure 5.15) showed no significant difference between the diet groups based on the significance level of 5%.

Table 5.13: Comparison of mean CS activity± Standard Error Mean of heart

	Control Feed	**Experimental Feed**	**P-value**
CS activity (µmol*min^{-1}*mg^{-1})	0.0363±0.01	0.0553±0.02	0.333
Number of samples (n)	10	10	

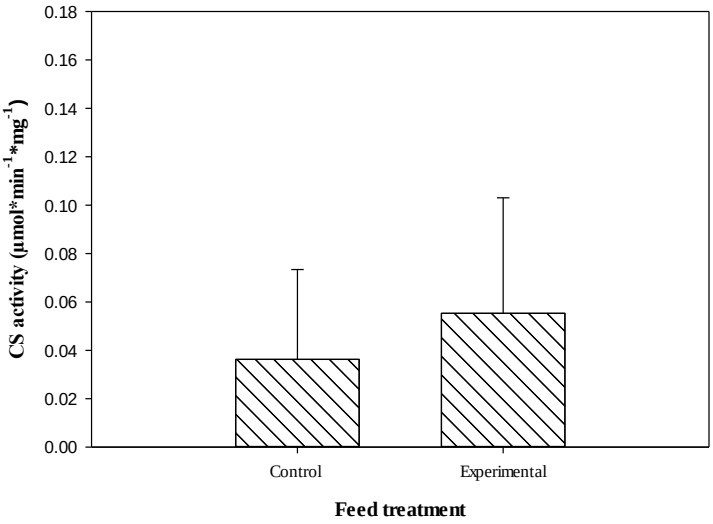

Figure 5.15: Mean values of CS activity in heart. Values are shown in µmol/(min*mg). The error bars represent standard deviation.

5.4.2 Liver tissue samples

Statistical analysis of CS activity in tissue slices of heart samples (table 5.14 and figure 5.16) showed no significant difference between the diet groups based on the significance level of 5%.

Table 5.14: Comparison of mean CS activity± Standard Error Mean in liver

	Control Feed	**Experimental Feed**	**P-value**
CS activity (µmol*min^{-1}*mg^{-1})	0.0063± 0.002	0.0141± 0.004	0.130
Number of samples (n)	10	10	

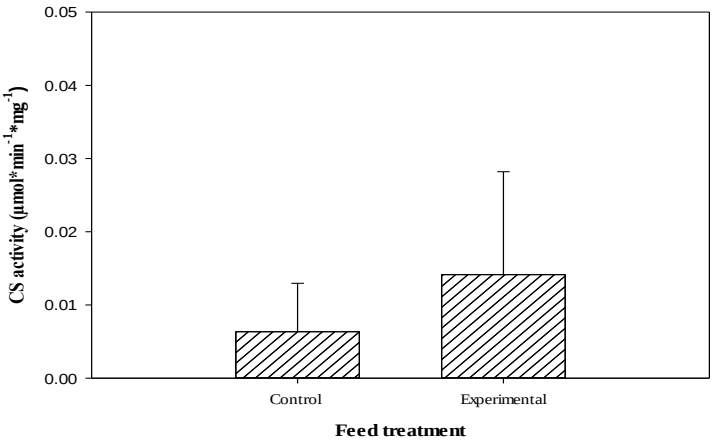

Figure 5.16: Mean values of citrate synthase activity in liver tissues. Values are shown in µmol/(min*mg). The error bars represent standard deviation.

5.4.3 CS activity per milligram of tissue protein

There was no statistically significant difference in CS activity normalized to protein content between the diet groups (figure 5.17) in heart (control: 0.0082±0.00262; experimental: 0.0164±0.00657; P value: 0.261) and liver (control: 0.000850±0.000219; experimental: 0.00269±0.000895; P value: 0.0611) tissues. Results are shown as mean values of CS activity±Standard Error Mean. Higher CS activity was observed in heart tissues compared to liver tissues.

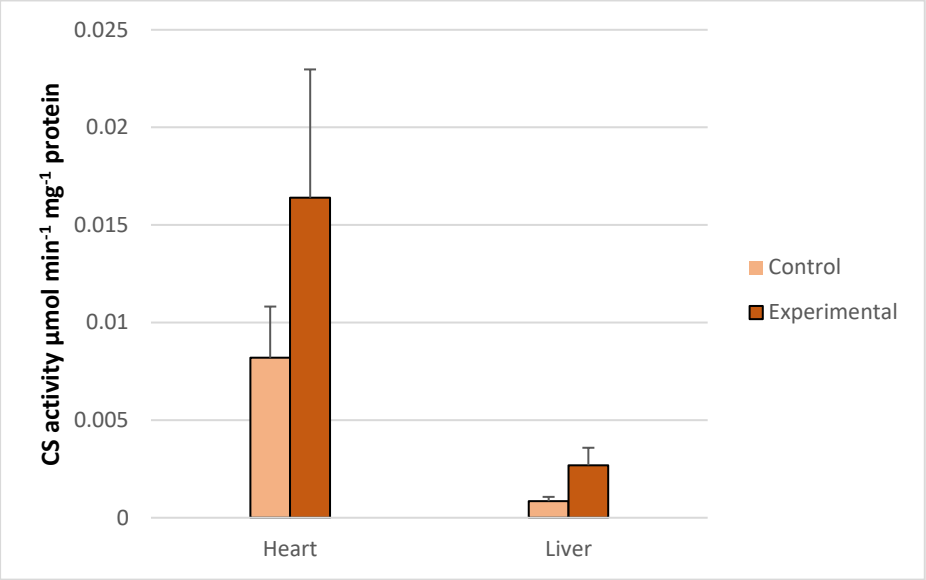

Figure 5.17: Mean CS activity per milligram tissue protein. Figure represents activity in heart and liver tissues between the diet groups. Error bars represent standard error mean.

6.0 Discussion

The present feeding experiment incorporated glutamate and succinate supplemented diets due to the promising results reported by a previous study (Oehme et al., 2010) on Atlantic salmon growth. Analysis from growth results in this experiment showed that the overall comparison of fish weight between the diet groups did not show any significant difference. Individual tank-based analysis of specific growth rate (SGR) did not show any statistically significant difference. Tank F fed with experimental diet showed the highest SGR percentage among all tanks. However, there were slight differences in SGR among tanks regardless of the diet provided. Tank A fed with experimental diet showed the lowest growth response. Though the reason behind this is unclear, there may be an effect between the tank placement and growth response. The fish in tank A may have been subjected to external disturbances due to its proximity to a larger tank assigned for another experiment. Experimental activities conducted in the larger tank may have affected the fish in tank A.

The flux response from succinate titration showed the maximum OXPHOS in HRR results, thus it was considered for OXPHOS calculations. The flux control ratios for heart and liver homogenates showed no significant difference between the diet groups.

It was evident that HRR analysis showed lower FCCP response in heart than in liver homogenates. There can be many reasons behind this observation. Lower FCCP response was also observed from another study (Hasli, 2015) conducted on Atlantic salmon. Furthermore, it was observed that the flux response of FCCP did not become stable even after several repeated titrations. Related results were shown by Hasli (2015). Another reason for the lack of response from FCCP could be the poor perfusion of the tissue than expected. This may have lead to reduced respiration from lowered partial pressure.

Results from CS activity showed lower enzyme activity in heart and liver. The reason behind this might be the lower oxidative capacity of mitochondria. Although the tissue samples were stored at -80°C instead of liquid nitrogen, it was found that CS activity can be preserved at subzero temperatures for longer periods of time (Shepherd and Garland, 1969), therefore the effect of storage method used for the tissues in sustaining the enzyme activity was ruled out. Furthermore, it was found that using larger amounts of tissues for CS activity can lead to lack of reaction itself (Z. Sumbalova (Ph.D.), 2018, personal communication, 13 February). It was revealed that the DTNB used in the protocol turns yellow after the reaction, yet an increase in absorbance will continue to occur. However, this increase in absorbance is related to post

reaction changes thus, not relevant for CS activity measurement. It is important to measure the linear absorbance increase at the start of the reaction. Moreover, it is necessary to minimize the time (<10 seconds) between the addition of oxaloacetate in the cuvette and measurement in the spectrophotometer. The use of plastic cuvettes for CS activity measurement was decided due to the wavelength (412 nm) proposed in the protocol (Brandt, 2010). It was reported that the amount of this enzyme is correlated with the ability of the cell to use oxygen (Moriyama and Srere, 1971). The CS activity results showed higher enzyme activity in heart tissues in comparison with liver, thus proving higher mitochondrial density present in the heart.

Interesting results were observed from ratio values between the substrates or inhibitors and succinate (maximum OXPHOS). These values confirmed that there was a significant effect from the diet thus, showing that responses from malate, cytochrome C and FCCP were diet dependent. Likewise, tissue-based comparison (i.e. heart vs liver) also confirmed that substrate responses are organ dependent. A further analysis using post-hoc tests to perform additional exploration of the differences among means was needed. However, a post-hoc test can only be performed at the presence of three or more means within each category. But due to the presence of only two means (i.e. control vs experimental diets, heart vs liver) in this experiment further analysis of differences between the means was not performed.

A normally distributed data is often obtained at the presence of a larger number of samples in an experiment according to the central limit theorem (McDonald, 2014). Due to a lesser number of samples achieving a normal distribution was a challenge in some data, therefore, a simple log transformation was used to achieve normal distribution. Non-parametric statistical methods were used to analyze data when normality was not achieved even after log transformation. However, better models with better predictions were achieved after most log transformations.

Obtaining of liver samples for homogenate preparation in HRR was a challenge since there was a necessity to take samples from the same portion of the liver consistently to get reliable results. This may have led to relatively higher standard deviations in liver HRR results than the heart. Improper shredding of samples may contain tissue particles present in the homogenate that may cause some disturbance in results. The initial dissolved oxygen concentration present in the sample at the beginning of a SUIT titration can affect the execution of the protocol in the sample. Rapid oxygen depletions were observed in some samples that lead to oxygen deficiency to continue the SUIT titration. Such samples had to be discarded and new samples were

prepared. However, the oxygen concentration never fell below 150 µmol/l during a proper SUIT titration procedure, therefore, should not lead to limited respiration.

Proper calibration of oxygraph equipment is vital to obtain reliable readings. Background calibration had to be performed several times in both oxygraph machines used for the experiments. It was a challenging task to get acceptable calibration readings from the machines. One of the electrodes had an issue with the calibration process since a relatively longer time was needed to reach stable flux during background calibration. Each sample run took a longer time than expected due to this reason. Any effort to fix this issue was not tried since repairing or cleaning of sensitive electrodes in oxygraph must be performed by experienced personnel to avoid any severe damage to the equipment.

7.0 Conclusions

Providing a specially formulated diet supplemented with of glutamate and succinate at 1% each for the smolt stage of Atlantic salmon resulted in a nominal increase in growth rate without a statistically significant difference. Mitochondrial respiration capacity analysis using high-resolution respirometry for heart showed a significant difference only for LEAK, whereas no significant difference was observed in liver samples. The previous study on FCCP response in salmon heart samples seemed to correlate with the current study in showing a lower response, thus raising the necessity of experimenting other uncouplers instead of FCCP to obtain a higher flux response. Further research is needed to study the effects of different uncouplers in Atlantic salmon.

The CS enzyme activity values reported in this study may have occurred due to the lower oxidative capacity of mitochondria in the tissues as discusses earlier. Higher CS activity in heart tissues than liver tissues confirmed higher mitochondrial density present in heart tissues which have been the case in other studies performed on salmonids.

Future studies could be conducted using different temperature regimes to determine the effect of mitochondrial respiration and feeding in glutamate and succinate supplemented diet in Atlantic salmon. Longer feeding periods along with studies focused on gut mitochondrial activity will facilitate in getting a better understanding of metabolism in Atlantic salmon. Few studies have been conducted on salmonids about mitochondrial activity therefore, there is a need for further understanding of the complex processes that take place in cells. Such studies will facilitate in providing a more efficient diet formula to obtain better growth, leading to increased production and sales in the expanding salmon industry in Norway.

References

Alberts, B., Bray, D., Hopkin, K., Johnson, A., Lewis, J., Raff, M., Roberts, K. and Walter, P., 2013. *Essential Cell Biology*. Garland Science.

Almaida-Pagán, P.F., Lucas-Sánchez, A. and Tocher, D.R., 2014. Changes in mitochondrial membrane composition and oxidative status during rapid growth, maturation and aging in zebrafish, Danio rerio. *Biochimica et Biophysica Acta - Molecular and Cell Biology of Lipids*, [online] 1841(7), pp.1003–1011. Available at: <http://dx.doi.org/10.1016/j.bbalip.2014.04.004>.

Alne, H., Oehme, M., Thomassen, M., Terjesen, B. and Rørvik, K.A., 2011. Reduced growth, condition factor and body energy levels in Atlantic salmon Salmo salar L. during their first spring in the sea. *Aquaculture Research*, 42(2), pp.248–259.

Alne, H., Thomassen, M.S., Takle, H., Terjesen, B.F., Grammes, F., Oehme, M., Refstie, S., Sigholt, T., Berge, R.K. and Rørvik, K.A., 2009. Increased survival by feeding tetradecylthioacetic acid during a natural outbreak of heart and skeletal muscle inflammation in S0 Atlantic salmon, Salmo salar L. *Journal of Fish Diseases*, 32(11), pp.953–961.

Archer, S.D. and Johnston, I. a, 1991. Density of cristae and distribution of mitochondria in the slow muscle fibers of Antarctic fish. *Physiological Zoology*, 64(1), pp.242–258.

Banh, S., Wiens, L., Sotiri, E. and Treberg, J.R., 2016. Mitochondrial reactive oxygen species production by fish muscle mitochondria: Potential role in acute heat-induced oxidative stress. *Comparative Biochemistry and Physiology Part - B: Biochemistry and Molecular Biology*, [online] 191, pp.99–107. Available at: <http://dx.doi.org/10.1016/j.cbpb.2015.10.001>.

Belding, D.L., 1934. The Spawning Habits of the Atlantic Salmon. *Transactions of the American Fisheries Society*, [online] 64(1), pp.211–218. Available at: <https://doi.org/10.1577/1548-8659(1934)64[211:TSHOTA]2.0.CO>.

Beveridge, M. and Grøttum, J.A., 2007. A review of cage culture: northern Europe. In: Halwart M, Soto D and Arthur J R, eds., *Cage Aquaculture: Regional Reviews and Global Overview. FAO Fisheries Technical Paper*, 1st ed. FAO, Rome, Italy, pp.129–158.

Bruce, A., Johnson, A., Lewis, J., Raff, M., Roberts, K. and Walter, P., 2002. *Molecular Biology of the Cell*. *Garland Science*, New York: Garland Science.

Burrells, C., Williams, P.D. and Forno, P.F., 2001. Dietary nucleotides: A novel supplement in fish feeds: 1. Effects on resistance to disease in salmonids. *Aquaculture*, 199(1–2), pp.159–169.

Burrells, C., Williams, P.D., Southgate, P.J. and Wadsworth, S.L., 2001. Dietary nucleotides: A novel supplement in fish feeds: 2. Effects on vaccination, salt water transfer, growth rates and physiology of Atlantic salmon (Salmo salar L.). *Aquaculture*, 199(1–2), pp.171–184.

Campbell, M.K. and Farrell, S.O., 2014. *Biochemistry*. Cengage Learning.

Chistiakov, D.A., Sobenin, I.A., Revin, V. V., Orekhov, A.N. and Bobryshev, Y. V., 2014. Mitochondrial aging and age-related dysfunction of mitochondria. *BioMed Research International*, 2014.

Cooper, G.M. and Hausman, R.E., 2007. *The Cell: A Molecular Approach*. *fourth edition*. Sinauer.

Desler, C., Hansen, T.L., Frederiksen, J.B., Marcker, M.L., Singh, K.K. and Juel Rasmussen, L., 2012. Is there a link between mitochondrial reserve respiratory capacity and aging? *Journal of Aging Research*, 2012.

Draxl, A., Eigentler, A. and Gnaiger, E., 2015. *PBI-Shredder HRR- Set : preparation of tissue homogenates for diagnosis of mitochondrial respiratory function*. OROBOROS Instruments Corp.

Drew, B., Phaneuf, S., Dirks, A., Selman, C., Gredilla, R., Lezza, A., Barja, G. and Leeuwenburgh, C., 2003. Effects of aging and caloric restriction on mitochondrial energy production in gastrocnemius muscle and heart. *American Journal of Physiology - Regulatory, Integrative and Comparative Physiology*, [online] 284(2), pp.R474–R480. Available at: <http://ajpregu.physiology.org/lookup/doi/10.1152/ajpregu.00455.2002>.

Egginton, S. and Sidell, B.D., 1989. Thermal acclimation induces adaptive changes in subcellular structure of fish skeletal muscle. *The American journal of physiology*, [online] 256(1 Pt 2), pp.R1-9. Available at: <http://www.ncbi.nlm.nih.gov/pubmed/2912202>.

Eigentler, A., Draxl, A., Wiethüchter, A., Kuznetsov, A. V, Lassing, B. and Gnaiger, E., 2015. Laboratory protocol: citrate synthase a mitochondrial marker enzyme. *Mitochondrial Physiology Network*, 4(3), pp.1–11.

Eya, J.C., Ashame, M.F. and Pomeroy, C.F., 2010. Influence of Diet on Mitochondrial Complex Activity in Channel Catfish. *Progressive Fish-Culturist*, 72(3), pp.225–236.

Eya, J.C., Ashame, M.F. and Pomeroy, C.F., 2011. Association of mitochondrial function with feed efficiency in rainbow trout: Diets and family effects. *Aquaculture*, [online] 321(1–2), pp.71–84. Available at: <http://dx.doi.org/10.1016/j.aquaculture.2011.08.037>.

Eya, J.C., Ashame, M.F., Pomeroy, C.F., Manning, B.B. and Peterson, B.C., 2012. Genetic variation in feed consumption, growth, nutrient utilization efficiency and mitochondrial function within a farmed population of channel catfish (Ictalurus punctatus). *Comparative Biochemistry and Physiology - B Biochemistry and Molecular Biology*, [online] 163(2), pp.211–220. Available at: <http://dx.doi.org/10.1016/j.cbpb.2012.05.019>.

Eya, J.C., Yossa, R., Ashame, M.F., Pomeroy, C.F. and Gannam, A.L., 2013. Effects of dietary lipid levels on growth, feed utilization and mitochondrial function in low- and high-feed efficient families of rainbow trout (Oncorhynchus mykiss). *Aquaculture*, [online] 416–417, pp.119–128. Available at: <http://dx.doi.org/10.1016/j.aquaculture.2013.08.022>.

FAO, 2016. *The State of World Fisheries and Aquaculture 2016*. [online] FAO. Available at: <http://www.fao.org/3/a-i3720e.pdf>.

Fasching, M., Renner-sattler, K. and Gnaiger, E., 2016. *Mitochondrial Respiration Medium - MiR06*. *Mitochondrial Physiology Network 14.13(06)*. OROBOROS Instruments Corp.

Fasching M and Gnaiger E, 2016. *Instrumental oxygen background correction and accuracy of oxygen flux*.

Fawcett, D.W., 1981. *The Cell*. W B Saunders Company.

Folmar, L.C. and Dickhoff, W.W., 1980. The parr—Smolt transformation (smoltification) and seawater adaptation in salmonids: A review of selected literature. *Aquaculture*, [online] 21(1), pp.1–37. Available at: <https://doi.org/10.1016/0044-8486(80)90123-4>.

Gnaiger, E., 2011. *The Oxygraph for High-Resolution Respirometry*. *Mitochondr Physiol*

Network 06.01. OROBOROS Instruments Corp.

Gnaiger, E., 2014a. *Mitochondrial Pathways and Respiratory Control - An Introduction to OXPHOS Analysis*. [online] *Mitochondrial Physiology Network*. Oroboros MiPNet Publications. Available at: <http://wiki.oroboros.at/images/f/fc/Gnaiger_2014_Mitochondr_Physiol_Network_MitoPathways.pdf>.

Gnaiger, E., 2014b. O2k calibration by DatLab. In: *Mitochondrial Physiology Network 19.01*. [online] OROBOROS Instruments Corp, pp.1–10. Available at: <www.bioblast.at/index.php/MiPNet19.01D_O2k-Calibration>.

Hartmann, N., Reichwald, K., Wittig, I., Dröse, S., Schmeisser, S., Lück, C., Hahn, C., Graf, M., Gausmann, U., Terzibasi, E., Cellerino, A., Ristow, M., Brandt, U., Platzer, M. and Englert, C., 2011. Mitochondrial DNA copy number and function decrease with age in the short-lived fish Nothobranchius furzeri. *Aging Cell*, 10(5), pp.824–831.

Hasler, A.D. and Wisby, W.J., 1951. Discrimination of Stream Odors by Fishes and Its Relation to Parent Stream Behavior. *The American Naturalist*, 85(823), pp.223–238.

Hasli, R.P., 2015. *Karakterisering av mitokondrierespirasjon og kvalitetsforskjeller på diploid og triploid atlantisk laks (Salmo salar L.) ved 5°C, 10°C og 15°C*. Norges miljø+og biovitenskapelige universitet.

Hendry, K. and Cragg-Hine, D., 2003. *Ecology of the Atlantic Salmon*. English Nature, Northminster House, Peterborough.

Hood, D.A., Zak, A.R. and Pette, D., 1989. Chronic stimulation of rat skeletal muscle induces coordinate increases in mitochondrial and nuclear mRNAs of cytochrome-c- oxidase subunits. *European Journal of Biochemistry*, 179, pp.275–280.

Hütter, E., Unterluggauer, H., Garedew, A., Jansen-Dürr, P. and Gnaiger, E., 2006. High-resolution respirometry-a modern tool in aging research. *Experimental Gerontology*, 41(1), pp.103–109.

Johnston, I.A. and Maitland, B., 1980. Temperature acclimation in crucian carp, Carassius carassius L., morphometric analyses of muscle fibre ultrastructure. *Journal of Fish Biology*, 17(1), pp.113–125.

Kontro, H., 2016. *Mitochondrial function and sirtuin expression in hippocampus of young and old high- and low-capacity runner rats*. University of Jyväskylä.

Kuznetsov, A. V, Veksler, V., Gellerich, F.N., Saks, V., Margreiter, R. and Kunz, W.S., 2008. Analysis of mitochondrial function in situ in permeabilized muscle fibers, tissues and cells. *Nature Protocols*, [online] 3(6), pp.965–976. Available at: <http://www.nature.com/doifinder/10.1038/nprot.2008.61>.

Lanza, I.R. and Nair, K.S., 2009. Functional Assessment of Isolated Mitochondria In Vitro. *Methods Enzymol*, 457(9), pp.349–372.

Lapajne, J., 2015. Detailed structure of mitochondrion. In: *Seminar Proceedings, University of Ljubljana*. pp.1–12.

Larsson, T., Koppang, E.O., Espe, M., Terjesen, B.F., Krasnov, A., Moreno, H.M., Rørvik, K.A., Thomassen, M. and Mørkøre, T., 2014. Fillet quality and health of Atlantic salmon (Salmo salar L.) fed a diet supplemented with glutamate. *Aquaculture*, [online] 426–427,

pp.288–295. Available at: <http://dx.doi.org/10.1016/j.aquaculture.2014.01.034>.

Li, P., Mai, K., Trushenski, J. and Wu, G., 2009. New developments in fish amino acid nutrition: Towards functional and environmentally oriented aquafeeds. *Amino Acids*, 37(1), pp.43–53.

Lodish, H., Berk, A., Kaiser, C.A., Krieger, M., Scott, M.P., Bretscher, A. and Ploegh, H., 2007. *Molecular Cell Biology*. 6th editio ed. W. H. Freeman.

Logan, D.C., 2006. The mitochondrial compartment. *Journal of Experimental Botany*, 57(6), pp.1225–1243.

Lugert, V., Thaller, G., Tetens, J., Schulz, C. and Krieter, J., 2016. A review on fish growth calculation: multiple functions in fish production and their specific application. *Reviews in Aquaculture*, [online] 8(1), pp.30–42. Available at: <http://doi.wiley.com/10.1111/raq.12071>.

Lyngstad, T.M., Hellberg, H., Viljugrein, H., Bang Jensen, B., Brun, E., Sergeant, E. and Tavornpanich, S., 2016. Routine clinical inspections in Norwegian marine salmonid sites: A key role in surveillance for freedom from pathogenic viral haemorrhagic septicaemia (VHS). *Preventive Veterinary Medicine*, [online] 124, pp.85–95. Available at: <http://dx.doi.org/10.1016/j.prevetmed.2015.12.008>.

McDonald, J.H., 2014. *Handbook of Biological Statistics*. 3rd ed. [online] Sparky House Publishing, Baltimore, Maryland. Available at: <http://www.biostathandbook.com/index.html>.

Meijer, A.J., 2003. Amino Acids as Regulators and Components of Nonproteinogenic Pathways. *The Journal of Nutrition*, [online] 133(6), p.2057S–2062S. Available at: <https://academic.oup.com/jn/article/133/6/2057S/4688224>.

Mills, D., 1991. *Ecology and Management of Atlantic Salmon*. Springer.

Moriyama, T. and A. Srere, P., 1971. of Rat and Rat Liver Citrate Synthases. *The Journal of Biological Chemistry*, 246(10), pp.3217–3223.

Neu, J., Shenoy, V. and Chakrabarti, R., 1996. Glutamine nutrition and metabolism: where do we go from here ? *FASEB journal : official publication of the Federation of American Societies for Experimental Biology*, [online] 10(8), pp.829–37. Available at: <http://www.ncbi.nlm.nih.gov/pubmed/8666159>.

Oehme, M., Grammes, F., Takle, H., Zambonino-Infante, J.L., Refstie, S., Thomassen, M.S., Rørvik, K.A. and Terjesen, B.F., 2010. Dietary supplementation of glutamate and arginine to Atlantic salmon (Salmo salar L.) increases growth during the first autumn in sea. *Aquaculture*, [online] 310(1–2), pp.156–163. Available at: <http://dx.doi.org/10.1016/j.aquaculture.2010.09.043>.

OpenStax College, 2013. *Biology*. [online] Rice University, Houston, Texas. Available at: <https://openstax.org/details/books/biology>.

Renner, K., Amberger, A., Konwalinka, G., Kofler, R. and Gnaiger, E., 2003. Changes of mitochondrial respiration, mitochondrial content and cell size after induction of apoptosis in leukemia cells. *Biochimica et Biophysica Acta - Molecular Cell Research*, 1642(1–2), pp.115–123.

Rørvik, K.A., Alne, H., Gaarder, M., Ruyter, B., Måseide, N.P., Jakobsen, J. V, Berge, R.K.,

Sigholt, T. and Thomassen, M.S., 2007. Does the capacity for energy utilization affect the survival of post-smolt Atlantic salmon, Salmo salar L., during natural outbreaks of infectious pancreatic necrosis? *Journal of Fish Diseases*, 30, pp.399–409.

Sedgwick, S.D., 1982. *The salmon handbook: the life and cultivation of fishes of the salmon family.* Andre Deutsch Ltd., London.

Shearer, W.M. and Balmain, K.H., 1967. Greenland Salmon. *Salmon and Trout Mag*, pp.239–244.

Shepherd, D. and Garland, P.B., 1969. The kinetic properties of citrate synthase from rat liver mitochondria. *The Biochemical journal*, 114(3), pp.597–610.

Terada, H., 1990. Uncouplers of oxidative phosphorylation. *Environmental Health Perspectives*, 87, pp.213–218.

Thorpe, J.E., Adams, C.E., Miles, M.S. and Keay, D.S., 1989. Some Influences of Photoperiod and Temperature on Opportunity for Growth in Juvenile Atlantic Salmon, Salmo salar L. *Aquaculture*, 82, pp.119–126.

Tyler, S. and Sidell, B.D., 1985. Changes in mitochondrial distribution and diffusion distances in muscle of goldfish upon acclimation to warm and cold temperatures. *Journal of Experimental Zoology*, [online] 232(1), pp.1–9. Available at: <http://doi.wiley.com/10.1002/jez.1402320102> [Accessed 3 Mar. 2018].

Vadder, F. De, Kovatcheva-Datchary, P., Zitoun, C., Duchampt, A., Fredrik, B. and Mithieux, G., 2016. Microbiota-Produced Succinate Improves Glucose Homeostasis via Intestinal Gluconeogenesis. *Cell Metabolism*, 24, pp.151–157.

Waterborg, J.H., 2002. The Lowry Method for Protein Quantitation. In: Walker J.M., ed., *The Protein Protocols Handbook*. [online] Humana Press, pp.7–10. Available at: <http://www.springer.com/978-0-89603-940-7>.

Williams, R.S., Salmons, S., Newsholme, E.A., Kaufman, R.E. and Mellor, J., 1986. Regulation of nuclear and mitochondrial gene expression by contractile activity in skeletal muscle. *The Journal of Biological Chemistry*, [online] 261(1), pp.376–380. Available at: <http://eutils.ncbi.nlm.nih.gov/entrez/eutils/elink.fcgi?dbfrom=pubmed&id=3941082&retmode=ref&cmd=prlinks%5Cnpapers2://publication/uuid/A428EE5B-8F3B-4BBE-BA59-A760720FEC46>.

Yamashita, S.I., Jin, X., Furukawa, K., Hamasaki, M., Nezu, A., Otera, H., Saigusa, T., Yoshimori, T., Sakai, Y., Mihara, K. and Kanki, T., 2016. Mitochondrial division occurs concurrently with autophagosome formation but independently of Drp1 during mitophagy. *Journal of Cell Biology*, 215(5), pp.649–665.

Appendix 1

Fish growth data

The following tables represent the fish weight data including initial weights before the feeding trial and final weights after the feeding trial. G&S represents glutamate and succinate diet. Tanks 8,9 and 14 were provided with glutamate and succinate diet and tanks 10, 11 and 12 were fed control diet.

	First weighing: 19.09.2017			**Start feeding**: 20.09.2017				**End weighing:** 26.10.2017			(starved on day)		
	G&S	G&S	control	control	control	G&S		G&S	G&S	control	control	control	G&S
Fish↓ tank →	**8**	**9**	**10**	**11**	**12**	**14**		**8**	**9**	**10**	**11**	**12**	**14**
1	99	94	104	114	101	101		164	170	228	201	149	171
2	110	92	145	114	96	93		125	165	227	207	210	183
3	103	82	87	93	125	98		178	167	178	144	153	257
4	83	125	122	89	112	97		197	211	160	224	196	207
5	91	107	96	93	110	111		223	153	216	124	212	203
6	104	115	92	79	114	87		210	240	194	168	177	192
7	103	100	78	125	95	119		186	148	246	140	179	219
8	128	116	95	110	102	98		162	188	216	196	166	181
9	80	99	107	89	112	102		260	214	208	205	205	196
10	97	121	113	88	105	111		169	176	175	183	163	164
11	88	80	85	123	90	96		232	206	275	196	184	167
12	98	77	115	89	114	100		203	194	202	156	217	183
13	91	82	110	76	114	105		245	197	255	200	179	181
14	101	120	105	91	102	101		192	218	206	150	183	215
15	100	99	111	94	137	96		161	155	190	163	169	179
16	130	107	115	119	114	116		206	171	163	215	189	198
17	121	108	141	93	101	87		198	208	162	205	173	189
18	117	104	99	102	84	118		184	198	205	143	177	176
19	106	93	102	103	100	90		205	164	176	147	192	164
20	113	121	101	102	95	92		152	168	207	153	180	144
21	101	90	111	93	105	127		224	194	234	240	186	200
22	120	106	133	105	139	91		185	202	193	198	195	182
23	144	85	132	114	118	102		148	164	194	174	231	205
24	109	91	112	81	115	104		156	155	173	180	165	167
25	121	84	89	105	102	97		167	154	183	203	189	175
26	84	108	125	131	85	95		210	220	198	196	264	169
27	109	107	106	105	106	107		211	195	220	195	204	178
28	93	118	111	96	101	93		190	134	199	222	226	172
29	99	108	143	97	101	89		154	228	148	180	227	187
30	114	89	91	86	90	109		152	211	147	153	217	213
average	**102.1**	**98.0**	**106.0**	**97.1**	**103.1**	**98.3**		**188.3**	**185.6**	**199.3**	**182.0**	**191.9**	**187.2**